ISLAMIC UNIVERSITY OF TECHNOLOGY

ORGANIZATION OF ISLAMIC COOPERATION

VIBRATION ANALYSIS OF A CRACKED CANTILEVER FLAT PLATE

B.Sc. Engineering (Mechanical) Thesis

AUTHORED BY:

SHAWKAT ISLAM
Student ID: 151433

SUPERVISED BY:

PROF. DR. MD. ZAHID HOSSAIN

Head, Department of Mechanical and Production Engineering

Islamic University of Technology (IUT)

Department of Mechanical and Production Engineering (MPE)

Islamic University of Technology (IUT)

NOVEMBER 2019

CERTIFICATE OF RESEARCH

The thesis title "**VIBRATION ANALYSIS OF A CRACKED CANTILEVER FLAT PLATE**" submitted by **SHAWKAT ISLAM (151413)** has been accepted as satisfactory in partial fulfillment of the requirement for the Degree of Bachelor of Science in Mechanical and Production Engineering on November, 2019.

Supervisor

PROF. DR. MD. ZAHID HOSSAIN

Head, Department of Mechanical and Production Engineering (MPE)

Islamic University of Technology (IUT)

DECLARATION

This is to clarify that the work presented in this thesis is an outcome of the analysis, simulation, experiment and research carried out by the author himself under the watchful supervision of Prof. Dr. Md. Zahid Hossain.

Authors

SHAWKAT ISLAM (151433)

Supervisor

PROF. DR. MD. ZAHID HOSSAIN

Head, Department of Mechanical and Production Engineering (MPE)

Islamic University of Technology (IUT)

ACKNOWLEDGEMENTS

I would like to express my deepest appreciation and sincere thanks to my respectable supervisor Prof. Dr. Md. Zahid Hossain, Head, Department of Mechanical and Production Engineering (MPE) for his support, guidance, care, tutelage, motivation and patience throughout the research period. His support and encouragement provided throughout this academic year is gratefully appreciated. Without his help and contribution my work would not have been able to come to this stage as it is right now. I feel very much obliged and indebted to Nagib Mehfuz, Lecturer, Department of Mechanical and Production Engineering (MPE) for his enormous support and guidance in making our research work successful. Apart from them we would like to thank each and every faculties of Department of Mechanical and Production Engineering (MPE) for their knowledge, assistance, motivation and care throughout the study period.

I also place on record, my sense of gratitude to one and all, who directly or indirectly, have lent their hands in successful completion of this project work. Finally, I want to express my gratitude to Allah, The Almighty.

ABSTRACT

This paper investigates the opportunities of observing the response of a cantilevered flat plate through vibration analysis using Eddy-Current Displacement sensors. External disturbance such as excitations, fluctuating loads etc. in plates causes vibration problem. Coupled bending and torsional motion is found in vibration analysis of cantilevered flat plates. It has been observed previously that with the increase in crack or slit length, natural frequency of a plate structure decreases. Here, non-linear vibration response for different crack position and length are to be inspected in relevance with similar works of other authors and also using finite element method for cross verification. Eddy-Current displacement sensors are used for measuring very small changes in displacement. Different types of root-slit are inspected numerically and experimentally. The output from the sensor are compared with available data. The linear free vibration response of cracked flat plate is measured using FEM calculation. The veering seen in between the higher modes of different crack models are also assessed. Errors found in the finite element analysis is also corrected and pointed out. The results validate the use of eddy-current displacement sensors in addition with the possibility of using FEM calculations for crack detection in a given structure.

Keywords: Flat plate, Vibration analysis, Modal analysis, Crack propagation, Crack type variation, Harmonic Analysis, Crack length variation, Veering between modes.

Table of Contents

List of Figures

List of Tables

1 Introduction

Among other commonly used structures such as rods, beams, shells and plates etc., flat Plates are used in all kinds of constructions such as stern structures, machinery, automobiles, tanks, buildings, ships, submarines, space vehicles, airplane, bridge decks etc. As these thin and light structures are used in numerous occasions in heavy structures to sensitive structures where it is subjected to fluctuating loads, engine vibration or other types of external forces that creates fatigue cracks, cracked flat plate structures, these areas have been studied and analyzed rigorously. In this work, the non-linear vibrational response of cracked flat plates is studied in order to observe and analyze cracks using finite element method and eddy-current displacement sensor. The natural frequency or free vibration of thin Aluminum flat plates are of primary interest due to its regular use in constructions and also due to availability of research papers on this material. In this study, modal and harmonic analysis of the plate is done, the veering between modes is observed. In modal analysis using FEM based software such as ANSYS and COMSOL Multiphysics, some error in the data found is pointed out, analyzed and removed from study. The result found in this work is compared with previous and recent works in this sector and correspondence is established. This work, although, based solely on analysis, may further be used in many other cases such as new crack detection methods, evaluating previously existing crack detection procedure, crack prevention, crack handling etc.

Literature concerning fatigue cracks on structures are numerous. Although there have been many researches on these sectors, resources on experimental approach are less in number. Dynamic behaviors of different structures were immensely studied during 1960s-70s in power generation sector due to fatigue cracks development in these structures under heavy load. Dimarogonas[1] provides a comprehensive literature survey on dynamic behaviors of different structures with cracks.

2 Literature Review

Vibration response on different types of structures have been studied immensely over the years. Many of the research works are based on Turbomachinery. Due to high rotational speed, the surrounding materials sometimes buckle as the vibration reaches the modal frequencies. Crack formation and their response due to vibration has also been a very rigorously studied sector.

There have been numerous studies on the vibration response of different structures. Dimarogonas published an intensive review on papers based on vibration response of different structures i.e. beams, shells, shafts, plates, rotors etc. Flat plates have been first modeled as a homogeneous Fredholm integral equation of the first kind in the works of Lynn and Kumbasar[2]. This work has been further progressed by Stahl and Keer[3], where they solved for centrally located internal crack and for crack emanating from one end as dual series equation and reduced it to Fredholm Integral of the second kind. These papers have been very vital for researchers in this field, as these methods have been proven to be effective for natural frequency predictions and verifications.

Ali and Atwal[4] used Rayleigh's Method to predict Natural Frequency of a flat plate rectangular plate with a narrow cutout and verified the findings using finite element method. Huang et al.[5] used Ritz method to determine frequency of thick cracked plates using Mindlin's Plate theory. In their work, they have considered different crack inclination angles, crack length and depth of the plate, crack positioning i.e. central crack, side crack etc. for analysis. The changes in crack pattern also changes its nodal patterns have been portrayed.

Research based on experimental and practical effects of excitation in cracked flat plates are relatively less. One of the early works in this area is of Maruyama and Ichinomiya[6], where time-averaged holographic interferometry is used to detect natural frequency of a flat plate. In their experiment, the aspect ratio of the plate was 1.25 and four parallel types of crack and a centrally located crack were investigated. Slits of various inclination angle were also experimented. The results found validated that

parallel cracks decrease the natural frequency slightly with an increase in length irrespective of its orientation. The cracks with inclinations of $\alpha=60^{o}$ show slightly increased frequency than that of $\alpha>60^{o}$ and then decreases with the inclination angle increase.

Finite element method has been used in almost all of the recent studies. These methods have proven to be very reliable on verifying actual response of structures. M. Bachene et al.[7] effectively used extended finite element method for analysis of plates with discontinuities and for shear deformation and rotational inertia, Mindlin's plate theory was taken into account. They verified their works using the data of previous works of Stahl[2] and Liew[8]. They determined and analyzed the change in modal frequencies for a clamped square plate with different crack length to plate length ratio.

Tanmoy Bose and Amiya R Mohanti[9] used Ritz method along with finite element method software (ABAQUS) to validate the results found for mobility-based crack detection in plate. The harmonic response of plates with different crack to length ratio and several inclinations of crack have been analyzed. Forced response at different positions of a clamped square plate have been reviewed. The response patterns may be used to understand different types of crack and their effects on the plate.

Nan Tao et al.[10] used time-averaged electronic speckle pattern interferometry (ESPI) to investigate the non-linear characteristics of a cantilevered flat plate with narrow slit and verified it using finite element method software (ANSYS). Mode shapes of plates with variable crack length is analyzed. The work done in this paper is based mainly on Tao's paper, as the experimental and simulated data can easily be compared.

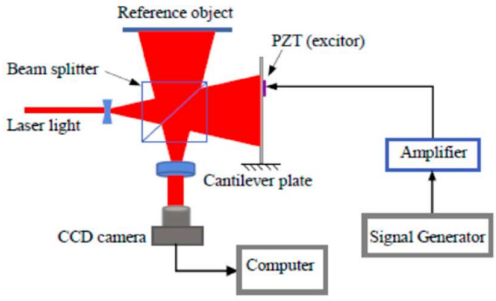

Figure 1: Experimental setup of the sensor by Nan Tao, Hanyang Jiang et al.

Acceleration based sensors are being used in some of the works to easily detect modal frequency of plates, such as in the work of Qiu, Wu and Ye[11], Andreaus and Baragatti[12] et al. Qiu, Wu and Ye have used PZT sensor in a side cracked cantilever plate and the response from the sensor is conditioned to have better control effects in vibration decay process and low amplitude vibration suppression. In Andreaus's work, using non-linear characteristics of forced vibration response cracked beams have been detected using acceleration-based sensor and analysis of FFT spectrum. They showed that, using bilinear frequency approximation, uncracked plate response and sub- or super harmonic component found in FFT (Fast Fourier Transformation) spectrum of the plate, crack determination is possible. Saito's[13] work states that curve veering is observed in plots of natural frequency vs crack length or crack position. Wider veering region entails continuously interchanging between modes and in cases of smaller veering region fast mode switching is present. To some extent, the veering is affected by non-linear characteristics due to closing of the crack. Otherwise, in general they are similar to those of the linear counterparts.

Although, this study is not based solely on crack detection methods, but this study may well be able to help in crack detection. As seen from the work of Nan Tao, Hanyang Jiang et al. they have used simulation and experimental procedure simultaneously for flat plates for non-linear response detection. Also, from the work of M. Elshamy, W.A. Crosby, M. Elhadary et al.[14] they have successfully used acceleration-based sensor for crack detection in a beam structure in addition with simulation for further verification.

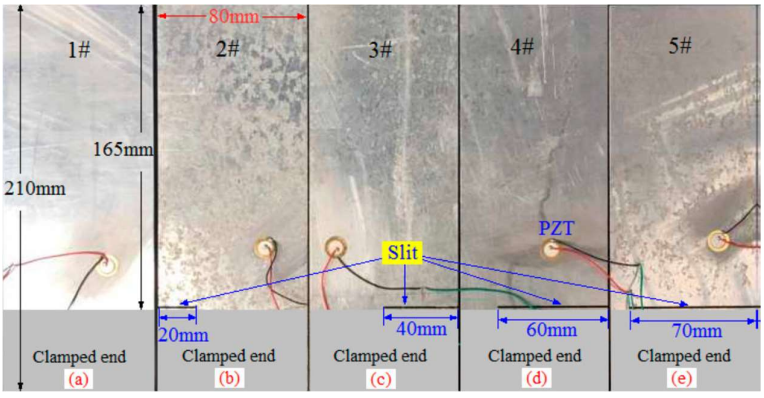

Figure 2: Experimental setup of the specimen by Nan Tao, Hanyang Jiang et al.

3 Methodology

SOLIDWORKS is used for modelling all the variants in the process for modal and harmonic analysis. These models are then exported into ANSYS for FEM analysis. For simulation ANSYS and COMSOL are both used. But in the work of Nan Tao, Hanyang Jiang et al. ANSYS Mechanical APDL is used. Both Multiphysics software provides good fit for a result, but the ANSYS has less error reproducing them. So, throughout the whole work ANSYS is used.

Using ANSYS, modal analysis, harmonic analysis is done. In the modal analysis the data obtained for various crack types are categorized plotted and analyzed. The mode shapes are also checked for better understanding. The modal frequencies are cross checked with previous work. The results are stored in Microsoft Excel and later graphs are produced from the data to understand effects of different crack types.

The modes are varied along crack position variation. The mode variations are cross-referenced with flat plate's modal frequencies and analyzed. Finally, this setup is tried experimentally to find accuracy in practical operations. While setting up this experiment, reduction of noise and external excitations must be removed.

4 Numerical Method

4.1 Modelling

The 3D model is prepared using SOLIDWORKS 2016. The cracks used in the models are rectangular slits of 1 mm width, varying length and 1.43 mm thick. Cracks are varied mainly in two directions:

Following Nan Tao's work, the specimen selected for experiment is an Aluminum flat plate of length 210 mm, width $b = 80mm$ and thickness $t = 1.43mm$. The free length of the plate is $a = 165mm$, while clamping 45 mm in a cantilevered state.

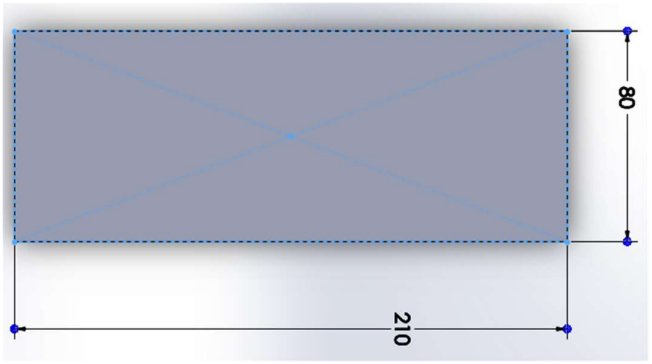

Figure 3: Unclamped dimensions of the flat plate model

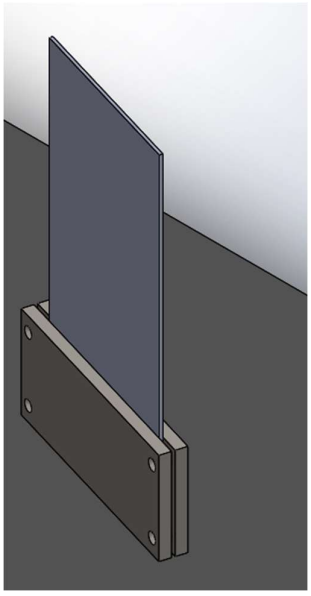

Figure 4: Clamped model of the flat plate positioned vertically with ground

Figure 5: Clamped portion removed of the flat plate model for simulation setup

Using FEM software (ANSYS) the models are tested using modal analysis and harmonic analysis. In the experiment the flat plate is clamped on one side and the deflection or displacement is determined using ECL 202e and the output is found in Oscilloscope. From the oscilloscope the output found are in Hz.

In the model of Figure 3, the flat plate is placed vertically with the ground to negate the effects of gravity on the data acquired. In certain cases, the effect gravity may lead to change in the natural frequency as well as mode shapes of the structure.

1. Horizontal with clamp edge: Varied from the clamped edge to free edge

    i. 70mm ii. 60mm iii. 40mm iv. 20mm

2. Vertical with clamp edge: Varied from left to right along the width

    a. Along clamped edge:

        i. 41.25mm ii. 82.5mm iii. 123.75mm

    b. Along free edge:

        i. 41.25mm ii. 82.5mm iii. 123.75mm

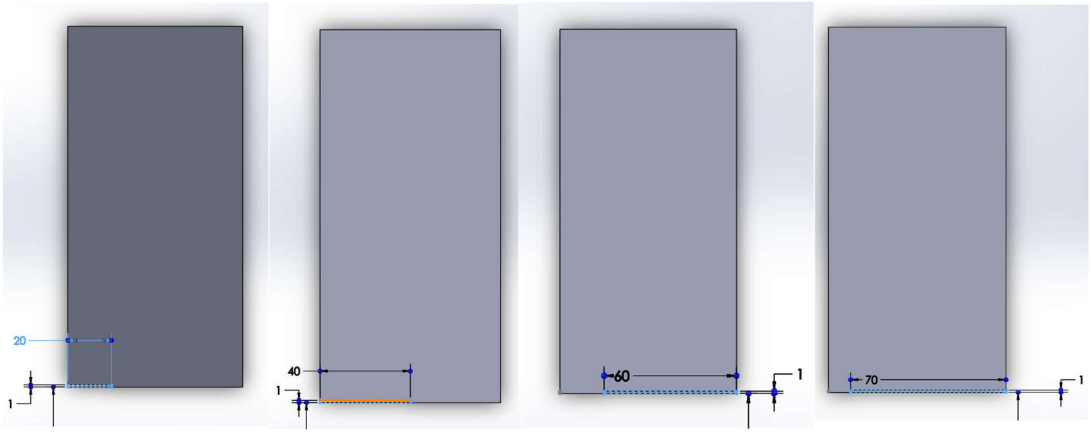

Figure 6: Root-slit of length i) 20 mm, ii) 40 mm, iii) 60 mm, iv) 70 mm

For crack position change models are made where cracks are moved towards the free end by 5 mm for each model and imported into ANSYS for modal analysis.

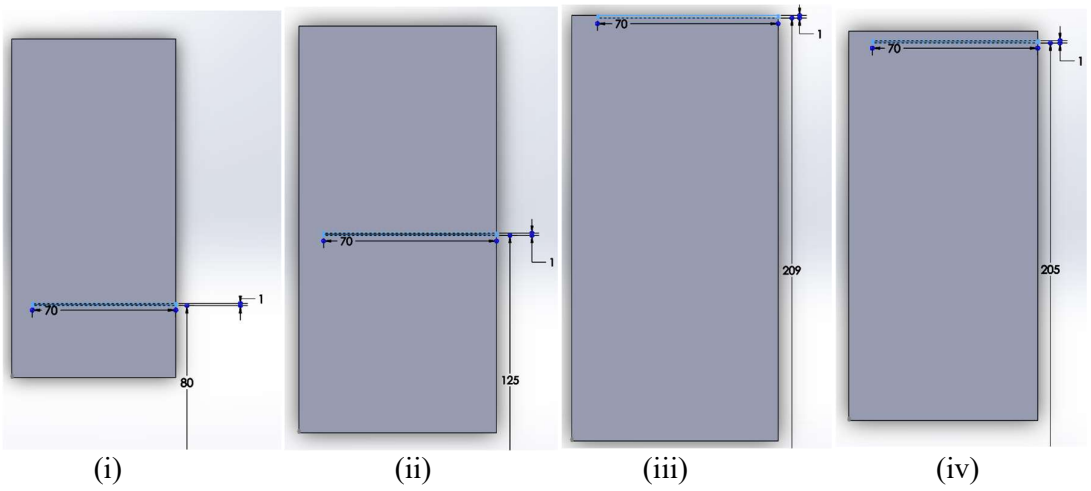

Figure 7: Model for crack position variation towards free end direction (bottom edge clamped) at i) 35 mm, ii) 70 mm, iii) 205 mm, iv) 209 mm

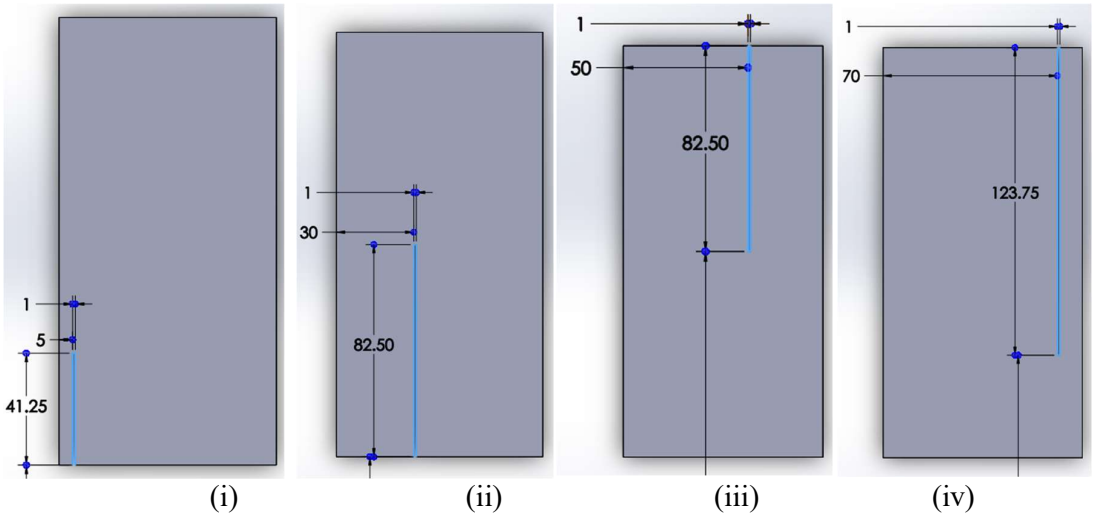

Figure 8: Crack position variation for vertically positioned crack of i) 41.25mm, ii) 82.5mm length along clamped end at clamped edge and of iii) 82.5 mm, iv) 123.75mm length at the free edge.

4.2 Meshing

Meshing determines the degree of freedom for the system. Higher degree of freedom gives better and more accurate results. For this analysis, meshing has been set to 2 mm for element size. This meshing produces results that are comparably similar with that of Tao's work.

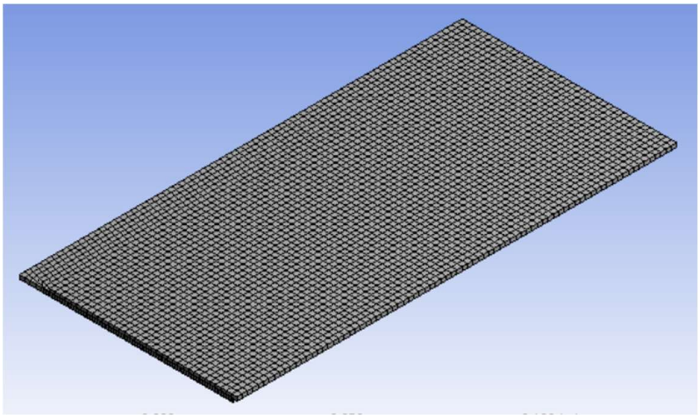

Figure 9: 2 mm element size used for meshing and clamped end boundary is set

4.3 Material Selection

Different material behaves differently under excitation. For this model, physical and geometric parameters used in FEM analysis are Young's modulus E = 70 GPa, Poisson's ratio, $\nu = 0.33$, mass density $\rho = 2770$ kg/m^3. Material selection is given in the Mechanical APDL section as Aluminum Alloy. As in this work, eddy-current sensor is being used, it can only detect small displacements in ferrous and non-ferrous metals.

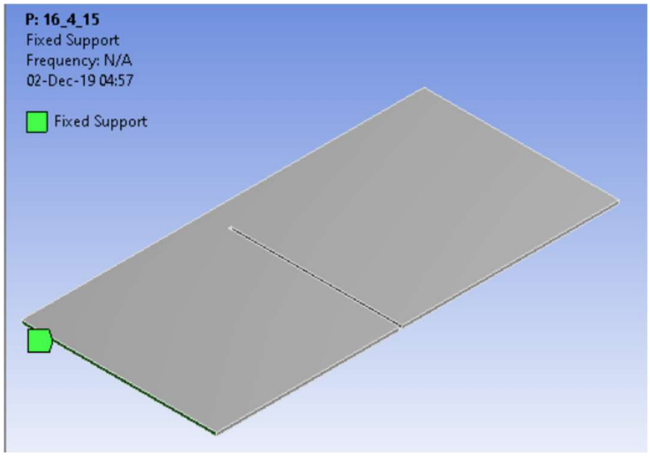

Figure 10: Boundary condition is set to fixed support at the face of removed portion of clamped edge

4.4 Modal Analysis

Modal analysis provides frequency for different modes of a structure. Variation in shape, size, thickness, physical properties and any type of external excitations effects the modes of a certain prototype or any other object for that matter. While analyzing this model in both ANSYS and COMSOL Multiphysics, it is seen that certain modes are actually not valid results. The mode shapes are also not valid as seen from the work of Nan Tao. So, the errors in all models were thoroughly checked. For each model first 14 to 15 modes were determined for all of the models. all of the models have a 5 mm difference of crack position in an orderly progression from end to end of the plate. All the crack modeled is of 1 mm width, 1.43mm thickness and varying length. The results obtained are tabulated and presented graphically along with the change in variation as follows:

Flat plate with no slit or crack:

Mode No.	Frequency,ω_n (Hz)
1	44.317
2	192.2
3	275.82
4	625.07
5	774.09
6	1197.8
7	1267
8	1532
9	1693.3
10	1973.3
11	2072.1
12	2356.5
13	2552.9
14	2972.6
15	3250.8

Table 1: Modal Analysis of Flat plate

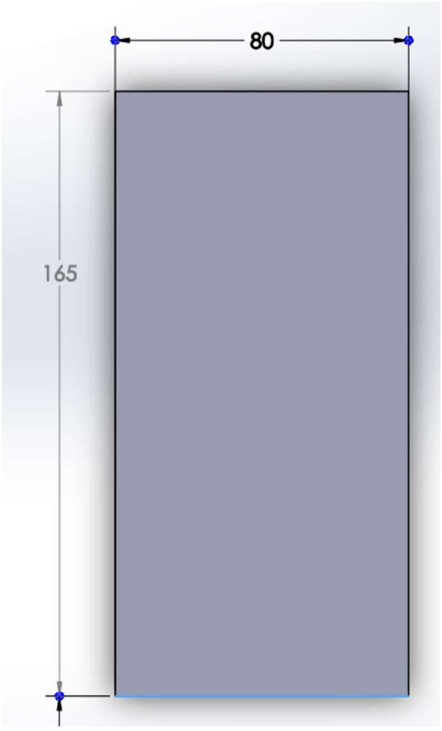

Figure 11: Flat Plate

This table is used further in this work for comparing the data found from cracked specimens of this same model. Below is the first 9 mode shapes of the structure in Figure 12. The mode shapes are used to evaluate the shifting in between various crack types. The mode shapes are seen throughout this work as from clamped end at the bottom of the figure and free end at the top of the figure. In the mode shapes the displacement regions are varied from low to high in eight order defined in colors respectively in the order Navy, Indigo, Blue, Cyan, Green, Lemon, Yellow, Red.

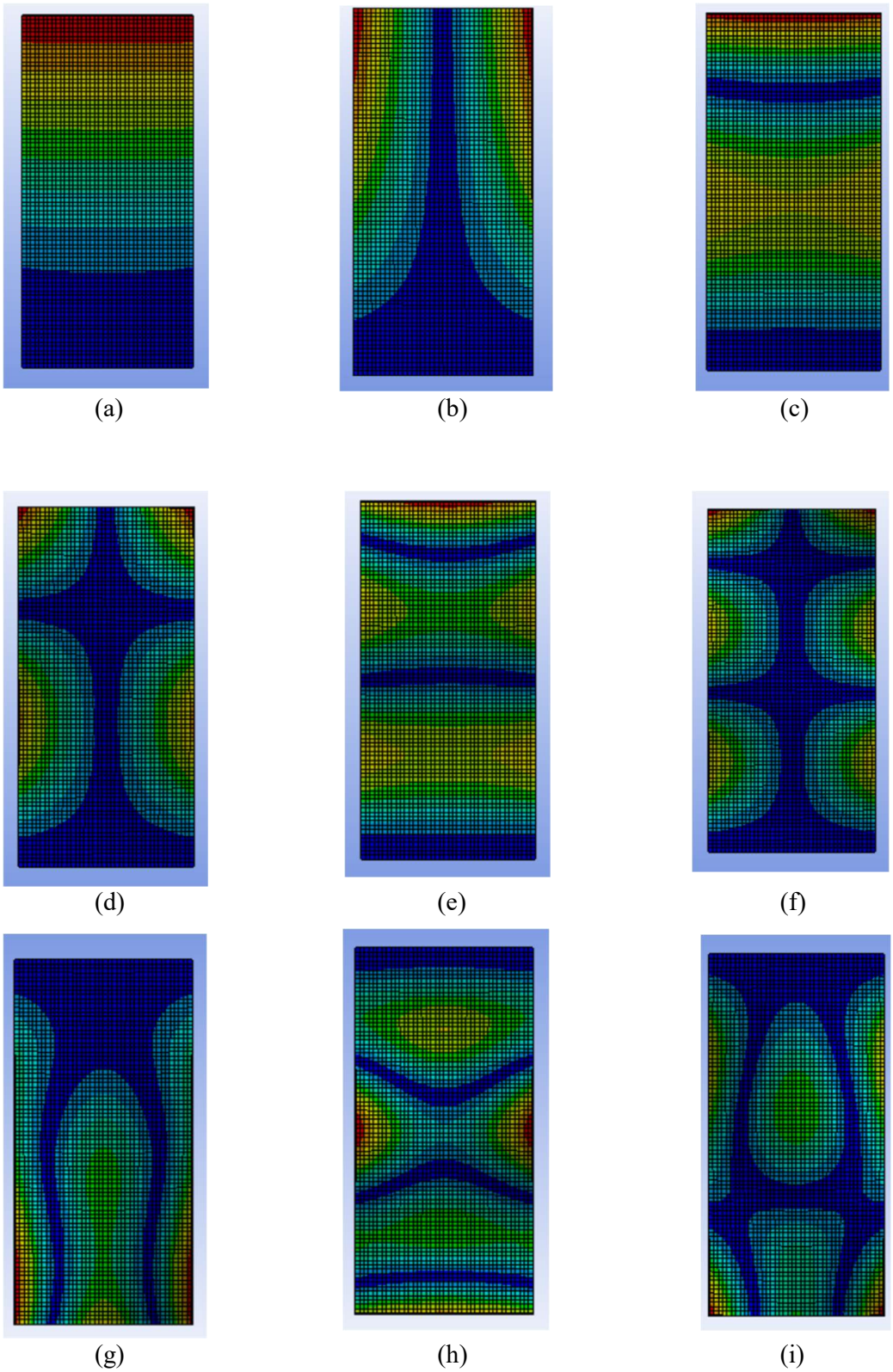

Figure 12: First 9 mode shapes of an intact flat plate model [(a) to (i)]

20mm crack length horizontal with the clamped end:

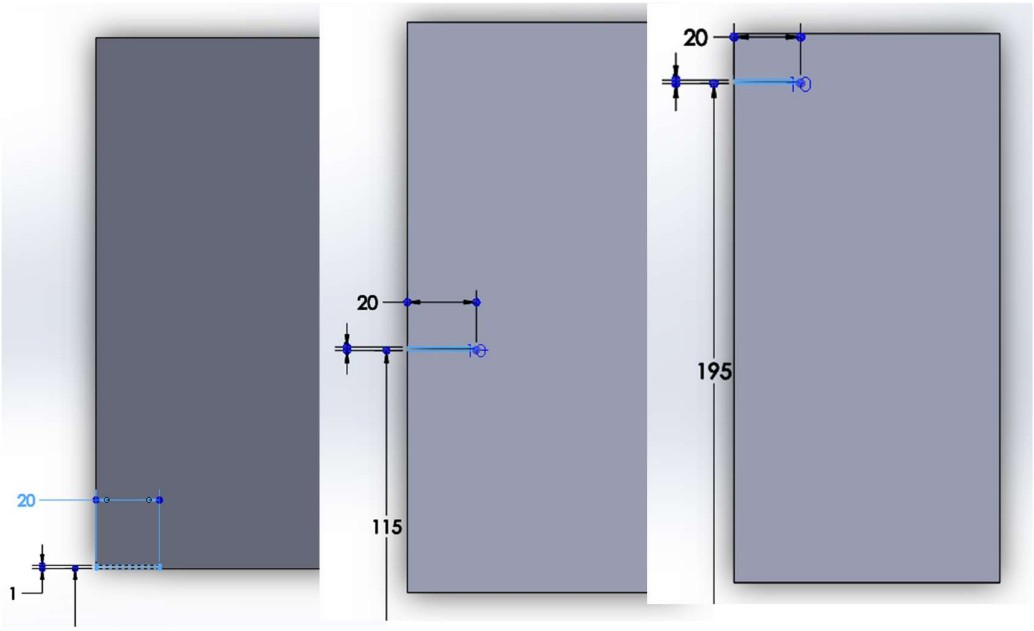

Figure 13: 20mm crack length horizontal with the clamped end

	1	2	3	4	5	6	7	8	9	10	11
1	42.744	42.096	41.757	41.674	41.736	41.881	42.061	42.257	42.454	42.647	42.83
2	182.68	181.35	181.48	181.8	181.93	181.89	181.78	181.69	181.65	181.7	181.83
3	266.64	265.3	266.02	267.74	269.59	271.18	272.25	272.75	272.66	272.07	271.07
4	590.36	587.42	589.52	592.13	594.25	596.23	598.37	600.87	603.64	606.55	609.3
5	749.23	749	753.06	757.7	760.51	760.79	758.62	754.98	750.96	747.68	745.75
6	1114.2	1110	1115.9	1123.7	1131.8	1140.8	1149.9	1157.8	1162.3	1161.6	1155
7	1259.8	1259.4	1259.4	1259.3	1259.3	1259.3	1259.3	1259.2	1259.4	1260.3	1262
8	1481.4	1483	1492.4	1499.7	1501.1	1496	1485.7	1473.5	1462.3	1454.7	1451.7
9	1616.6	1611.9	1614.9	1621.6	1630.1	1639.3	1649.1	1660	1671.5	1682.7	1690.9
10	1846.3	1847.5	1859.3	1873.9	1889.2	1902.6	1908.3	1898.5	1870.4	1835.8	1810.7
11	2235.1	2240.4	2261.4	2285.2	2303.8	2310.7	2306.8	2299.5	2294.4	2296.7	2302.6
12	2415.2	2422	2434.6	2444.2	2449.9	2454.4	2444.7	2401.8	2361.5	2352.4	2364.8
13	2727.9	2746.3	2780.9	2821.5	2860.7	2873.7	2795.1	2712.1	2701.2	2721.1	2753.7
14	3111.5	3133.6	3160.3	3180.5	3191.1	3197.3	3186.6	3171	3171.9	3161	3121.4

(a)

	12	13	14	15	16	17	18	19	20	21	22
1	43.004	43.165	43.316	43.454	43.581	43.694	43.798	43.889	43.971	44.042	44.104
2	182.05	182.35	182.72	183.16	183.65	184.18	184.75	185.35	185.97	186.59	187.22
3	269.82	268.43	267.05	265.79	264.76	264.01	263.6	263.53	263.82	264.43	265.32
4	611.61	613.16	613.71	613.1	611.33	608.53	604.97	600.98	596.91	593.1	589.83
5	745.48	746.61	748.72	751.06	752.94	753.69	752.96	750.69	747.24	743.17	739.26
6	1144.3	1132.3	1122.1	1115.4	1113.4	1115.9	1122.5	1132.1	1142.8	1152.5	1158.3
7	1264	1265.7	1266.3	1265.7	1263.9	1261.2	1257.8	1254.4	1251.4	1249.2	1248.8
8	1452.9	1456.6	1461.2	1465.2	1467.9	1468.9	1467.2	1461.6	1452.2	1441.1	1431.6
9	1692.9	1689.7	1684.8	1680.3	1676.1	1671.9	1668.1	1665.6	1664.4	1663.2	1659.9
10	1804.2	1815.3	1838.3	1867.5	1894.1	1899.7	1881.4	1860.3	1846.8	1841.8	1844.4
11	2298.8	2271.7	2217.9	2151.6	2098.1	2087.3	2126.2	2191.2	2260	2308.7	2317.7
12	2388.9	2417.6	2446.2	2469.6	2483.4	2485.7	2479.6	2470.5	2464.8	2463.5	2459.3
13	2799.1	2856.2	2842.4	2796	2770.5	2761.5	2764	2776.8	2803.2	2805.3	2752.4
14	3043.4	2954.3	2979.9	3091.3	3195.6	3211.1	3152.7	3044.5	2922.2	2875.7	2968.6

(b)

	23	24	25	26	27	28	29	30	31	32	33
1	44.157	44.203	44.241	44.273	44.3	44.323	44.343	44.36	44.375	44.389	44.401
2	187.85	188.47	189.06	189.64	190.19	190.7	191.18	191.61	191.99	192.32	192.57
3	266.43	267.69	269.02	270.34	271.58	272.7	273.66	274.46	275.11	275.65	276.09
4	587.35	585.84	585.46	586.31	588.49	592.03	596.91	603	609.95	617.11	623.51
5	736.2	734.64	734.92	737.18	741.18	746.47	752.38	758.32	763.85	768.78	772.92
6	1158.1	1152	1142	1130.5	1119.8	1111.8	1108.5	1112.1	1125.3	1149.9	1182
7	1250.3	1253.3	1256.5	1259.3	1261.4	1262.9	1264.2	1265.3	1266.3	1267.2	1268.1
8	1426.1	1425.8	1429.9	1437	1445.6	1454.7	1463.2	1470.9	1480.2	1496.4	1520.7
9	1653.3	1643.7	1633	1623.1	1615.7	1611.8	1611.7	1615.6	1624.1	1641.9	1677.4
10	1853.1	1866.7	1882.6	1895.1	1895.3	1879.7	1856	1832.5	1814.6	1811.4	1866.6
11	2284.8	2229.2	2173.7	2134.1	2122.8	2143.3	2182.6	2217.5	2227.4	2216.3	2227.4
12	2457.7	2465.5	2474.5	2475.4	2463.4	2440.9	2414.5	2393.5	2385.4	2385.4	2387.9
13	2731.2	2727.5	2733.8	2751.8	2784.7	2832.1	2849.6	2788.2	2733.9	2689.4	2649.6
14	3086.3	3175.2	3212.6	3172	3067.1	2964.4	2926.7	2998.8	3066.6	3095.6	3076.4

(c)

Table 2: Modal analysis of variation in crack position of 20mm crack length horizontal with the clamped end (a), (b) & (c)

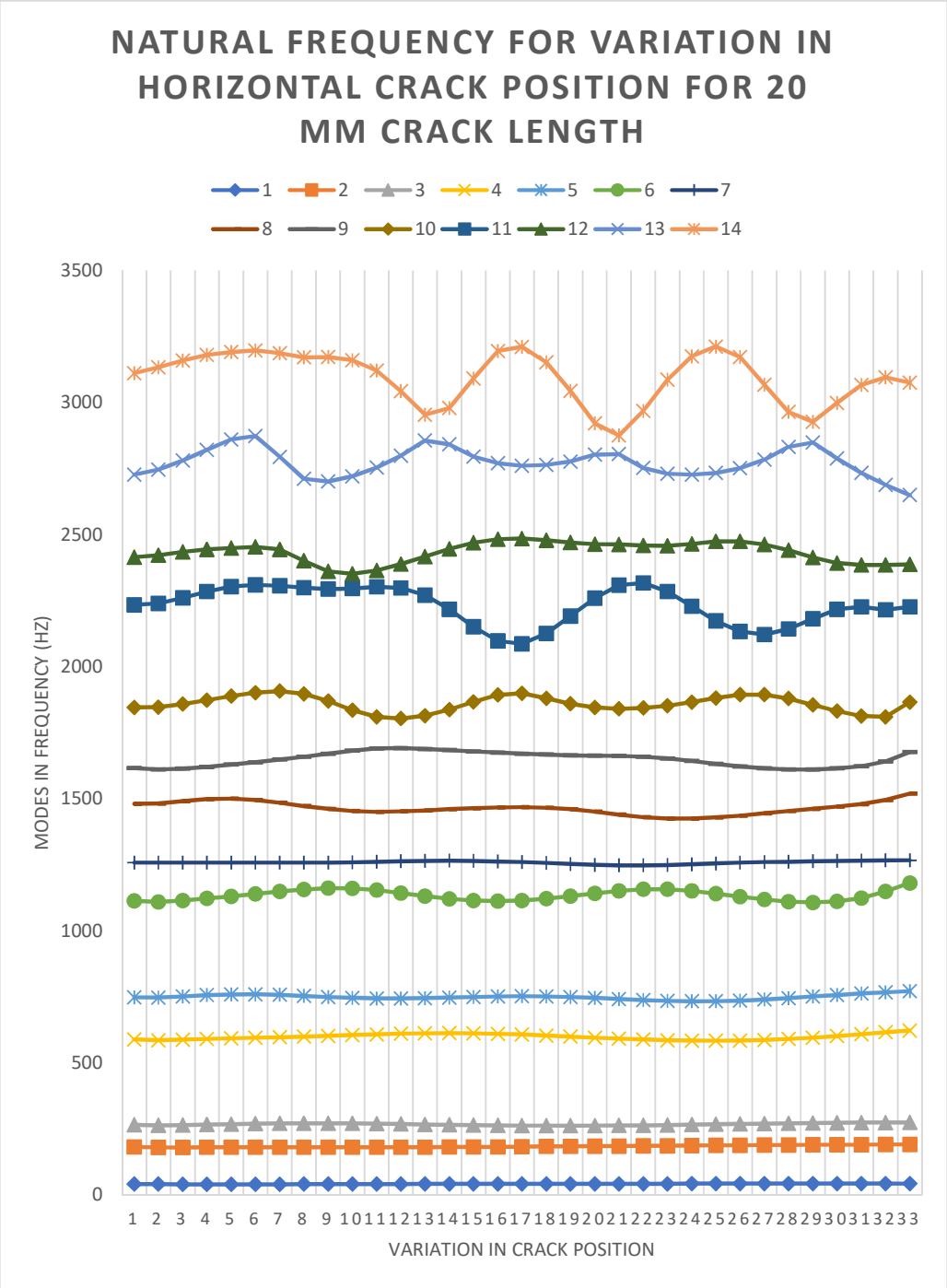

Figure 14: Modal analysis of variation in crack position of 20mm crack length horizontal with the clamped end

The table (a), (b) & (c) are of three parts of one entire table of which the rows indicate the modal frequencies of each mode for respective flat plate model with crack or very thin rectangular slit, and the columns indicate the variation of crack position of the same length along one side of the plate to the other side. So, the first characteristics that could be seen from the variation of different crack position on the table columns is that no data is exactly like the other one. This is true for all the cracked models of horizontally placed cracks along the clamp. In the models with cracks vertically placed along the clamp, similarities can be found, but that is due to the symmetry in the positioning of the crack.

For this 20 mm crack length the variations in different modes can be better understood from the graphical representation of the data which is shown in Figure 14. In the graph, each mode is assigned a line which progresses along with the variation in crack position. As we know that in higher modes the frequency usually varies more than usual, this can also be seen from the graph, in higher modes the fluctuations may be seen as simple waves that varies along the crack position. For this small crack, the variations are although not neglectable, but also not very great.

The mode shapes are also shown for variation in modes due to crack position change. For this the positions selected throughout the work are at the clamped edge, midway to the free edge and near the free end for horizontally placed cracks along the clamped edge. These position in the table are 1^{st}, 16^{th} & 33^{rd} in the columns respectively for this type of variation of horizontally placed cracks. For vertically placed cracks along the clamped edge only at one side and in the middle the mode shapes are shown. The 2^{nd}, 6^{th} and 9^{th} modes are shown for all of the variations for a better evaluation and observation.

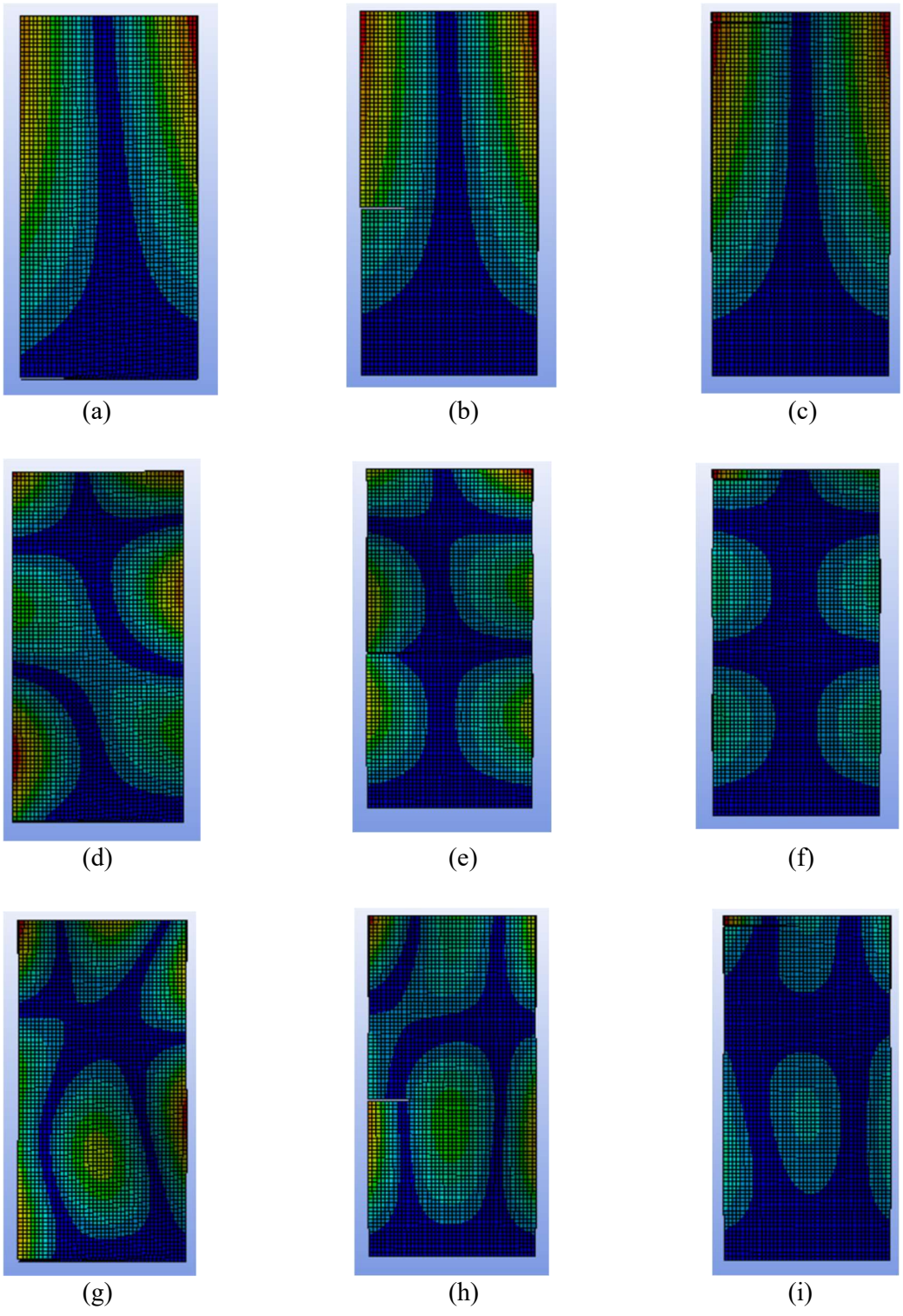

Figure 15: Mode shapes of 2nd [(a), (b) & (c)], 6th [(d), (e) & (f)] & 9th [(g), (h) & (i)] mode of crack length 20mm

40mm crack length horizontal with the clamped end:

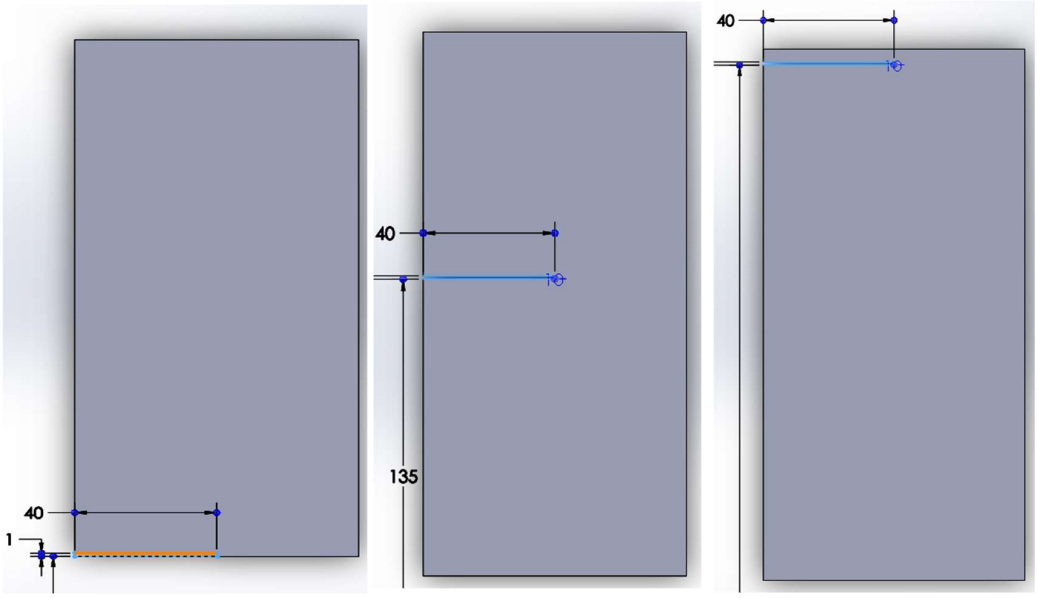

Figure 16: 40mm crack length horizontal with the clamped end

	1	2	3	4	5	6	7	8	9	10	11
1	38.382	37.007	36.345	36.138	36.225	36.516	36.927	37.41	37.924	38.453	38.979
2	159.45	156.31	154.9	153.8	152.89	152.18	151.69	151.47	151.54	151.93	152.59
3	249.78	248.56	249.94	252.46	255.33	258.02	260	260.96	260.72	259.33	256.91
4	490.32	486.23	488.41	493.13	500.07	509.09	519.95	532.46	546.19	560.58	574.8
5	704.15	705.09	709.05	713.08	715.93	716.93	715.63	712.19	706.83	699.59	689.48
6	899.43	914.44	938.08	966.68	998.67	1032.7	1067.5	1101.8	1131.3	1039.9	958.31
7	1252.7	1255	1256.4	1257.1	1257.5	1257.6	1256.9	1251.4	1163.9	1169.9	1201.4
8	1315.8	1333.2	1353.1	1372.3	1389.7	1402.9	1398.9	1322.4	1266.1	1263.1	1262.2
9	1531.3	1554	1579.1	1598.6	1609.9	1612.4	1597	1553.3	1552.6	1577.9	1607.3
10	1719.2	1731	1749.2	1775	1807.2	1843.5	1858.2	1703.2	1679.1	1678.2	1685.6
11	2053.9	2106.4	2165.1	2230.1	2275.6	2202.4	1891.2	1927.7	1976.5	2033.8	2102.1
12	2296	2288.7	2287.4	2284.6	2301.7	2372.6	2348	2336.2	2331.2	2324	2312
13	2592.9	2651.5	2708.3	2760.8	2810.2	2544.7	2478.1	2555.6	2623.8	2675.1	2707.2
14	3034	3091.7	3109.4	3124.8	3115.5	2863.6	2925.9	3007.6	3105.8	3085.4	3042.5

(a)

	12	13	14	15	16	17	18	19	20	21	22
1	39.497	39.998	40.482	40.941	41.376	41.781	42.158	42.501	42.814	43.092	43.34
2	153.51	154.66	156.02	157.55	159.22	161.02	162.93	164.9	166.94	169.03	171.16
3	253.76	250.18	246.53	243.08	240.09	237.72	236.11	235.32	235.37	236.23	237.85
4	587.67	596.92	596.64	582.4	562.35	542.38	524.33	508.65	495.49	484.79	476.47
5	675.2	657.94	645.85	646.34	653.23	661.06	667.73	672	673.14	671.04	666.42
6	910.3	890.6	891.96	906.63	928.39	952.33	974.97	994.37	1010.1	1021.3	1024.3
7	1232.3	1252.3	1251.4	1246.3	1238.8	1228.8	1215.3	1196.7	1172.5	1147.8	1132.8
8	1261.9	1272.2	1303.1	1337.1	1369.5	1388.8	1374.2	1337.1	1306.1	1287.6	1278
9	1629.9	1642.4	1648.1	1648.9	1637.2	1596	1581	1604.4	1631.6	1645.2	1645.3
10	1700.7	1720.6	1737.2	1738.8	1704.9	1680.4	1677.5	1680.2	1687	1697.5	1706.5
11	2182.6	2239.2	2102	1949.6	1877.1	1882.3	1923.4	1996.1	2106.1	2234.6	2215.3
12	2291.5	2266.6	2311.2	2313.4	2313	2316	2322	2329.4	2336	2335.6	2338.2
13	2695.3	2543	2497.3	2573	2643.9	2682.7	2693.1	2667.4	2574.6	2464	2525.6
14	2907.5	2838.5	2873.9	2958.2	3108.5	3185	3122.2	2973.4	2863.8	2840.6	2880.2

(b)

	23	24	25	26	27	28	29	30	31	32	33
1	43.555	43.741	43.9	44.034	44.145	44.239	44.316	44.381	44.435	44.482	44.521
2	173.32	175.51	177.71	179.91	182.08	184.19	186.2	188.05	189.69	191.07	192.15
3	240.11	242.88	246.03	249.41	252.94	256.56	260.26	264.06	267.93	271.73	275.15
4	470.35	466.16	463.54	462.12	461.65	462.29	464.75	470.5	482.3	505.55	553.79
5	660.65	655.49	652.52	652.85	656.61	662.74	669.24	674.04	675.97	675.01	672.92
6	1014.7	996.54	976.06	956.51	938.81	922.62	906.6	888.99	868.47	844.37	815.61
7	1135.6	1153.6	1179.6	1208.7	1235.5	1251.7	1257.9	1260.5	1261.8	1258.4	1232.8
8	1273.2	1271.2	1271.1	1272.9	1278.8	1291.7	1301.9	1298.1	1283.4	1266.6	1266.1
9	1634.2	1611.5	1579.4	1543.9	1513.2	1497.2	1504.7	1530.3	1554.5	1564.4	1556.9
10	1712.2	1718	1727.1	1740.4	1755.7	1762.8	1756.5	1744	1728.9	1713.3	1701.3
11	2107.3	2012.9	1941.1	1891.9	1867.8	1882.4	1950.8	2069.3	2144.8	2084.5	2026.8
12	2339.2	2334.7	2328.5	2322.1	2315.8	2305.1	2274.6	2217.7	2197.9	2277.8	2332.9
13	2637.6	2671.9	2666.7	2637.1	2585.4	2526.1	2499.9	2546.1	2618.9	2630.7	2603.9
14	3022.8	3148.8	3189.7	3047.3	2931.8	2862.1	2830.4	2844.5	2937.2	3023.6	3046.9

(c)

Table 3: Modal analysis of variation in crack position of 40mm crack length horizontal with the clamped end (a), (b) & (c)

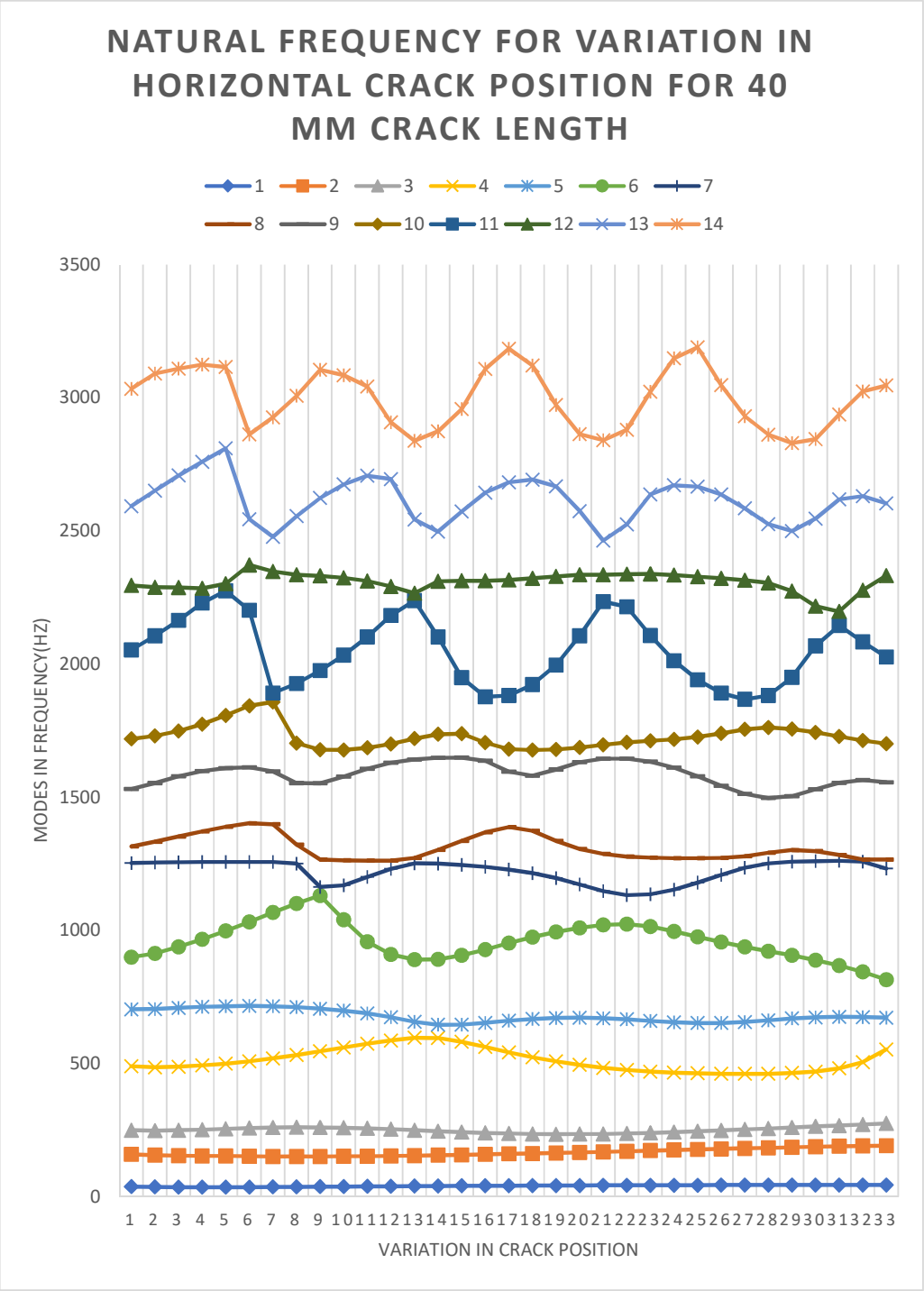

Figure 17: Modal analysis of variation in crack position of 40mm crack length horizontal with the clamped end

The data in this table is of the flat plate with a 40 mm crack length horizontally positioned along the clamp. The variations in this data table in contrast with the previous table shows that longer crack length shows more variation in the modal frequencies at higher modes which is true for the following models also. These variations along crack position change are greater than that of 20 mm crack length. There are also similar characteristics as the previous model, such as, extreme points can be seen in the variation from the graphs which indicates that a same crack length at a specific point in any structure may yield the highest or lowest natural frequency at any mode. Another point of interest is the shape of the mode lines in the graph for consecutive modes are often found similar in shape although in cases they may show opposing extreme points in between the lines. This evaluation is done solely by looking at the graphs, although they are never perfectly same, they have slight twitches arbitrarily on the line which other modes clearly does not have. So, the lines may not be modeled as easy as shifting phase between the modal lines from the data acquired from this analysis.

The mode shapes in this model shown can be distinguished from the mode shapes of the flat plate with no crack. The crack length is obviously shifting the mode shapes in every case. In the last figure of 9^{th} mode shape for the crack's position near the free end in Figure 18(i), the mode shape is shifted below the crack at the free end up to the clamped end. This mode shape however seems close to the mode shape of 8^{th} mode of the flat plate, although a slightly distorted due to the presence of the crack.

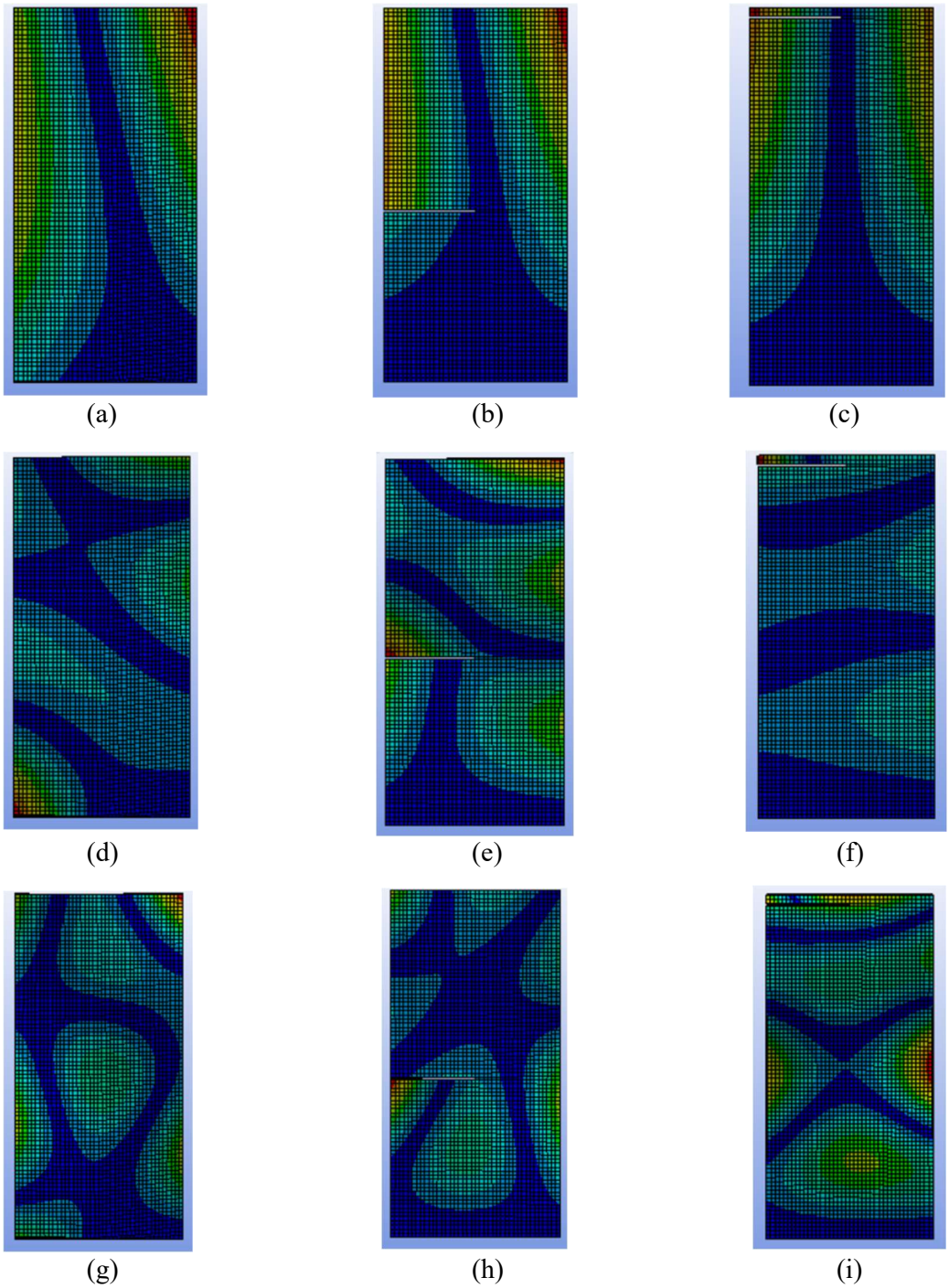

Figure 18: Mode shapes of 2nd [(a), (b) & (c)], 6th [(d), (e) & (f)] & 9th [(g), (h) & (i)] mode of crack length 40mm

60mm crack length horizontal with the clamped end:

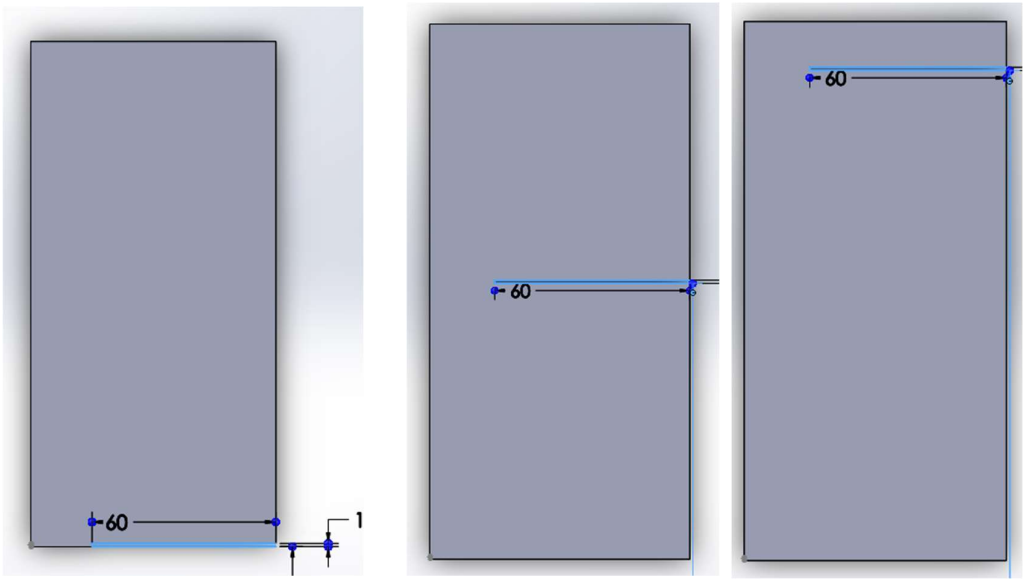

Figure 19: 60mm crack length horizontal with the clamped end

	1	2	3	4	5	6	7	8	9	10	11
1	31.084	29.148	28.439	28.316	28.519	28.943	29.515	30.192	30.937	31.729	32.55
2	122.16	116.99	113.52	110.95	109.33	108.52	108.37	108.73	109.52	110.68	112.17
3	229.43	228.45	230.55	233.67	236.91	239.82	241.96	243.02	242.72	240.93	237.67
4	385.5	389.15	397.39	408.89	423.27	440.16	459.24	480.16	502.37	524.78	545.09
5	660.45	661.23	665.41	669.48	672.08	672.78	671.31	667.63	661.04	648.91	625.04
6	816.49	847.23	883.81	924.32	966.88	1009.3	1048.7	1077.4	986.05	859.03	788.68
7	1219.7	1229.1	1242.3	1255.3	1256.5	1255.2	1253.1	1203.2	1128.6	1148.8	1167.2
8	1260.5	1259	1257.9	1257.5	1269.9	1287.4	1302.6	1250.4	1247.5	1245.8	1247.1
9	1475.4	1500.3	1522.6	1542.5	1562.1	1580.6	1579.4	1401.6	1432	1485.9	1540.6
10	1633.4	1659.2	1702.2	1750.6	1793.3	1824.7	1617.5	1613.4	1625.5	1638.3	1653.5
11	1927.4	1944.7	1976.5	2019.8	2075.8	2113.2	1869	1894.3	1922.1	1947.5	1965.4
12	2101.5	2138	2183.8	2235.1	2290.5	2217.8	2213	2263.5	2263.8	2194.1	2148.1
13	2556.7	2626.5	2686.5	2738.7	2781.6	2358	2427.6	2465.1	2419.2	2453.9	2527.3
14	2664	2731.4	2822.6	2916.6	3004.3	2830.5	2810.1	2680.2	2702.5	2760.1	2773.6

(a)

	12	13	14	15	16	17	18	19	20	21	22
1	33.391	34.243	35.099	35.951	36.793	37.616	38.415	39.18	39.906	40.585	41.213
2	113.94	115.99	118.29	120.82	123.56	126.48	129.52	132.62	135.72	138.75	141.69
3	233.17	227.76	221.88	215.97	210.45	205.65	201.84	199.24	197.98	198.12	199.61
4	554.88	531.19	497.31	467.34	442.17	421.14	403.66	389.22	377.55	368.52	362.14
5	595.14	592.62	601.73	610.46	618.25	625.04	630.36	633.22	632.36	626.65	615.96
6	768.24	778.87	807.13	845.42	887.37	925.15	948.72	949.98	932.12	907.32	884.8
7	1179.3	1184	1183	1178.4	1171.5	1162.6	1152.2	1142.4	1135.5	1131.2	1129.2
8	1254.2	1268.8	1289.8	1315.2	1341.7	1344.7	1298.9	1260.4	1242.3	1236.3	1235.5
9	1583.6	1607.6	1612.7	1593.3	1523.6	1466.7	1496.9	1546	1523.2	1505.9	1495.1
10	1672.4	1693	1705.3	1677.5	1630.8	1601	1572.9	1564.8	1633.1	1676.6	1688.2
11	1968.4	1950.8	1909.8	1859.9	1855.3	1863	1878.8	1918.8	2004.7	2139.8	2103.3
12	2152.9	2189.1	2073.1	1972.7	1950.9	1980.8	2043.4	2122.8	2207.9	2281	2301.2
13	2608.3	2380.2	2373	2496.1	2597.6	2641	2647.8	2629.3	2466.1	2313.5	2441
14	2669.8	2735.2	2827.5	2868	2986.1	3017.5	2853.3	2672.7	2615.2	2562	2526.9

(b)

	23	24	25	26	27	28	29	30	31	32	33
1	41.783	42.296	42.748	43.142	43.481	43.768	44.008	44.209	44.373	44.508	44.616
2	144.56	147.47	150.55	153.96	157.85	162.34	167.52	173.38	179.66	185.69	190.44
3	202.24	205.64	209.33	212.83	215.86	218.37	220.65	223.34	227.65	235.93	252.91
4	358.49	357.6	359.18	362.23	364.8	364.63	360.59	353.12	343.29	332.03	320.3
5	601.59	586.13	572.75	564.81	565.44	576.03	593.88	612.47	625.93	632.41	632.25
6	867.59	855.36	847	842.06	840.9	844.06	850.05	852.75	845.1	826.77	802.13
7	1129.5	1132.3	1136.7	1141	1143.9	1146	1150.7	1162.5	1179.6	1195.9	1204.8
8	1236.6	1238.6	1241.6	1245.7	1250.6	1254.7	1256.5	1257.3	1258.9	1260.9	1263.4
9	1490.5	1491.2	1494.7	1484	1444.9	1429	1453.6	1485.3	1490.6	1503	1533.2
10	1669.2	1622.2	1560.4	1516.1	1514.8	1516.6	1521.3	1577.5	1665	1688.5	1683.9
11	1997.6	1926	1885.2	1862.7	1850.4	1845.2	1850.4	1891.8	1894	1844.5	1835.1
12	2258.7	2192	2128.3	2075.9	2037.4	2010.8	1986.1	1949.5	2029.9	2064.6	2033.7
13	2543.2	2577.4	2568.3	2580.1	2503.9	2397.7	2301.5	2243.1	2311.9	2491	2437.5
14	2709.2	2916.7	3010.7	2902.7	2833.6	2809.3	2752.6	2665.8	2595.6	2661.5	2639.5

(c)

Table 4: Modal analysis of variation in crack position of 60mm crack length horizontal with the clamped end (a), (b) & (c)

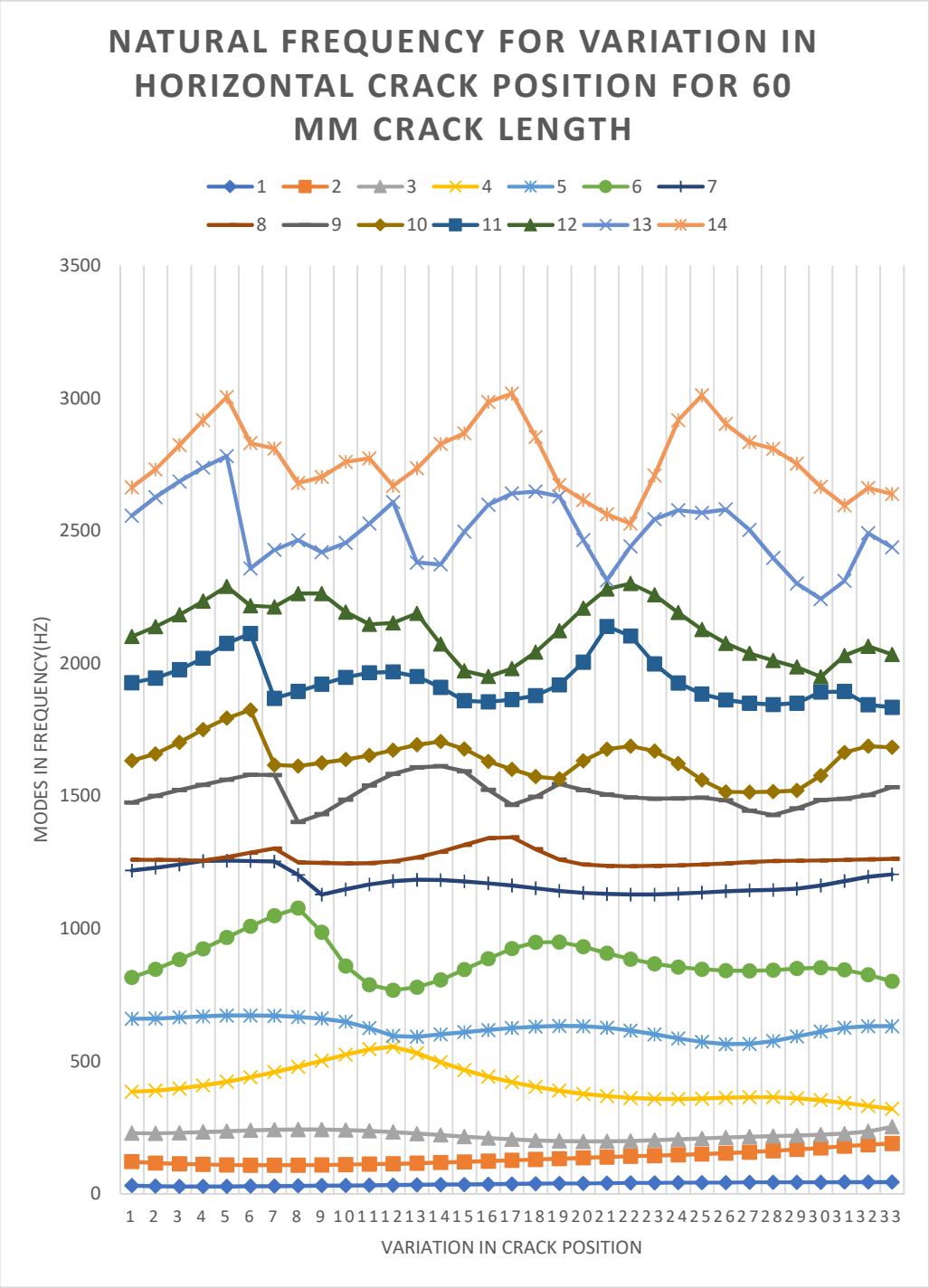

Figure 20: Modal analysis of variation in crack position of 60mm crack length horizontal with the clamped end

The data in this table is of the flat plate with a 60 mm crack length horizontally positioned along the clamp. This data set in higher modes is more chaotic than the previous two models. The variations among the mode lines in the graph between these three models indicate that longer crack length shows more extreme behavior in the shape of the line of modes among the flat plate models with crack position variation. Longer cracks show much more variation in the modes. The slight change between the lines of crack position variation for i.e. 14 th mode for all of the crack types are detectable.

The mode shapes for this model also show shifts in the mode shapes as seen from the mode shapes of the uncracked flat plate. The mode shapes have similarites in between the variations and the small change in the crack's position the effects seem to silghtly change the mode lines in the graph as well the mode shapes too. Although in longer crack shape the variations seem to be changing the shape of the mode lines and the mode shapes too, towards one extreme.

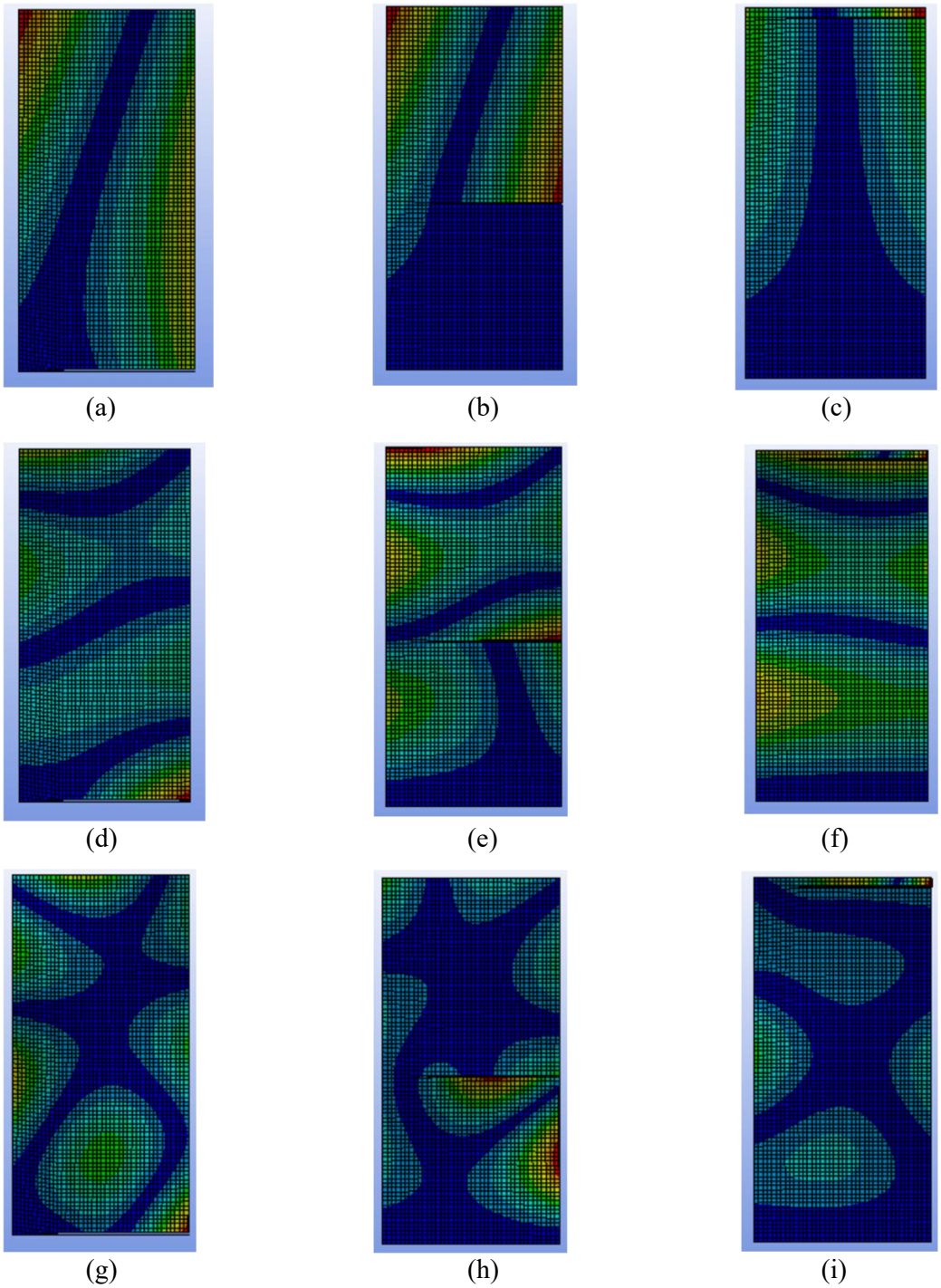

Figure 21: Mode shapes of 2nd [(a), (b) & (c)], 6th [(d), (e) & (f)] & 9th [(g), (h) & (i)] mode of crack length 60mm

70mm crack horizontal with the clamped end:

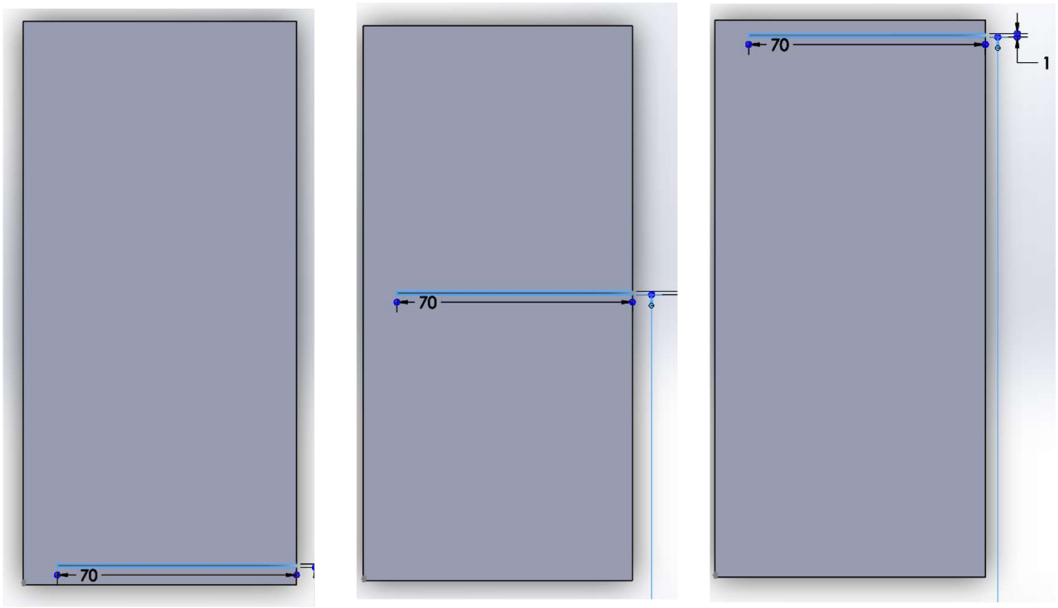

Figure 22: 70mm crack length horizontal with the clamped end

	1	2	3	4	5	6	7	8	9	10	11	12
1	25.656	23.5	22.973	23.01	23.326	23.824	24.452	25.176	25.974	26.827	27.727	28.665
2	98.117	90.92	86.68	84.514	83.653	83.599	84.089	84.975	86.182	87.667	89.411	91.403
3	216.31	215.45	218.49	222.42	226.26	229.57	231.97	233.15	232.85	230.91	227.27	222.11
4	351.23	357.43	368.8	383.66	401.15	420.89	442.73	466.44	491.39	515.75	532.99	520.65
5	632.9	632.28	637.45	642.53	645.77	646.66	645.08	641.12	634.14	621.29	598.17	586.13
6	798.63	833.19	874.19	918.84	964.75	1008.9	1046.8	1063.4	933.61	805.3	739.6	726.94
7	1143.3	1142.5	1151.8	1165	1183.2	1209.1	1242.4	1172.7	1123	1135.7	1141	1137.1
8	1253.1	1252.3	1254	1255.9	1256.1	1254.1	1249.4	1244.6	1235.9	1230.9	1234.5	1247.7
9	1425.8	1450.1	1477.9	1507.8	1537	1561.2	1528.2	1325.7	1379.7	1451	1520.6	1570.1
10	1581.2	1630.7	1692.4	1747.6	1785.5	1805.3	1582.7	1582.8	1579.5	1574.3	1573.3	1584.8
11	1823.9	1843.8	1879.8	1933.3	2007.4	2088.7	1845.6	1858	1861.6	1850	1841.5	1847.1
12	2072	2121.4	2177.9	2233.1	2282.6	2134.8	2172	2234.4	2171.2	2129.7	2129.3	2141.6
13	2523.5	2572.3	2623.8	2677	2728.2	2340.2	2372.4	2291.2	2299.4	2364.2	2444.3	2539.4
14	2574.1	2678.8	2795.3	2901.4	2985.8	2777.6	2663.5	2597.9	2681.9	2753.7	2754.8	2627.4

(a)

	13	14	15	16	17	18	19	20	21	22	23	24
1	29.635	30.631	31.65	32.683	33.725	34.766	35.799	36.812	37.796	38.74	39.634	40.468
2	93.641	96.125	98.852	101.82	105	108.34	111.76	115.13	118.25	121	123.34	125.42
3	215.71	208.55	201.13	193.94	187.42	181.93	177.79	175.31	174.73	176.22	179.69	184.73
4	484.25	449.26	419.99	396	376.26	359.93	346.39	335.31	326.51	320.07	316.22	315.46
5	592.74	599.9	605.65	610.71	615.23	618.73	620.17	618.08	610.84	597.63	579.28	558.4
6	745.71	782.61	829.73	879.99	923.24	944.79	934.15	900.76	863.61	833.31	812.25	799.09
7	1129	1121	1115.6	1114.1	1117.7	1124.2	1122.6	1117.2	1117	1118.4	1117.3	1112
8	1266.5	1287.9	1311.2	1334.6	1292.8	1219.6	1191.7	1194.8	1202	1207.6	1213.4	1221.3
9	1585.6	1582.7	1527.5	1421	1392.9	1445.2	1475.6	1435.6	1402.7	1382.7	1376.1	1380
10	1615.3	1644.4	1654.3	1626.3	1586.4	1537.8	1534.6	1612.5	1664.9	1678.1	1653.9	1596.3
11	1839.3	1778.8	1735.4	1782.1	1827.5	1828	1856.7	1933.8	2084	2049.6	1941.4	1877.2
12	2155.4	2066.3	1950.1	1874.8	1869.1	1960.1	2067.8	2179.4	2213.5	2297	2233.2	2141.8
13	2368.3	2337.8	2447.6	2535.1	2564.1	2563.8	2553.9	2403	2285.5	2348	2453.6	2489.8
14	2671.7	2752.8	2783.1	2907.3	2993.1	2818.7	2610.6	2543.8	2505.8	2458.6	2652.1	2896.7
15	2779.9	2816.3										

(b)

	25	26	27	28	29	30	31	32	33	34
1	41.233	41.924	42.537	43.071	43.525	43.905	44.213	44.458	44.643	41.233
2	127.51	129.9	132.9	136.8	141.96	148.79	157.82	169.73	184.39	127.51
3	190.55	196.17	200.72	203.8	205.5	206.24	206.54	207.27	211.84	190.55
4	318.29	324.83	333.54	340.45	341.31	335.61	325.46	312.57	296.97	318.29
5	538.32	522.7	516	523.53	547.12	578.84	605.71	621.85	628.4	538.32
6	791.61	788.51	789.79	796.8	810.97	828.37	835.29	824.57	802.52	791.61
7	1103.8	1095.4	1089.2	1086.5	1087	1088.3	1095.9	1120	1166.8	1103.8
8	1230.5	1239.7	1247.9	1253.7	1242.5	1248	1254.9	1258.8	1261.1	1230.5
9	1384.7	1364.3	1314.6	1271.2	1278.5	1345.9	1406.6	1382.5	1373.1	1384.7
10	1529.6	1493.1	1491.6	1490	1475.4	1454	1551.3	1668.9	1632	1529.6
11	1843.8	1824.5	1810.7	1797.9	1786.5	1781.1	1781.8	1731.9	1702.1	1843.8
12	2060.9	1999.8	1965.5	1958.2	1955.1	1923.6	1906.1	2026	2022.7	2060.9
13	2518.8	2518.7	2457.8	2356.3	2268.5	2224.3	2234.6	2418.4	2404.7	2518.8
14	2964.2	2830.7	2753.6	2736.6	2691.4	2603.8	2533.6	2571.7	2636.7	2964.2
15								2949.4	3012.3	

(c)

Table 5: Modal analysis of variation in crack position of 70mm crack length horizontal with the clamped end (a), (b) & (c)

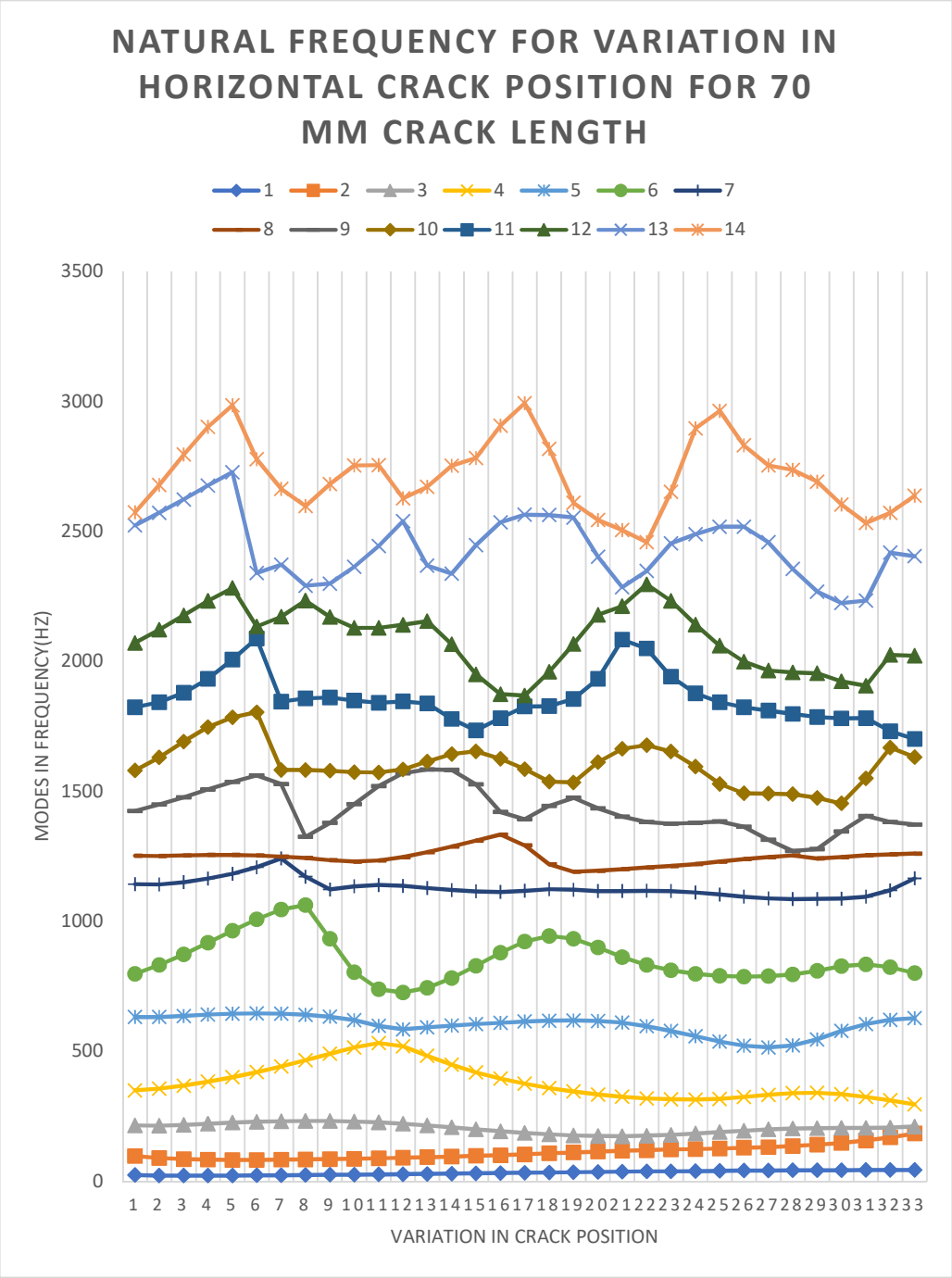

Figure 23: Modal analysis of variation in crack position of 70mm crack length horizontal with the clamped end

The data in this table is of the flat plate with a 70 mm crack length horizontally positioned along the clamp. This data set shows similar characteristics and type of variations as previously discussed. The shape of the lines of modes among the variations between crack position are more extreme than all the previous models discussed.

The mode shapes of this model show shifting of mode shapes in accordance with the crack's position and length as seen previously from other models. The changes seen in these mode shapes according to previous models are mentioned already. It is noticed from the variation between the shapes that the from the crack's position to the free end the behavior is more towards the extreme than from the clamped end to the crack's position.

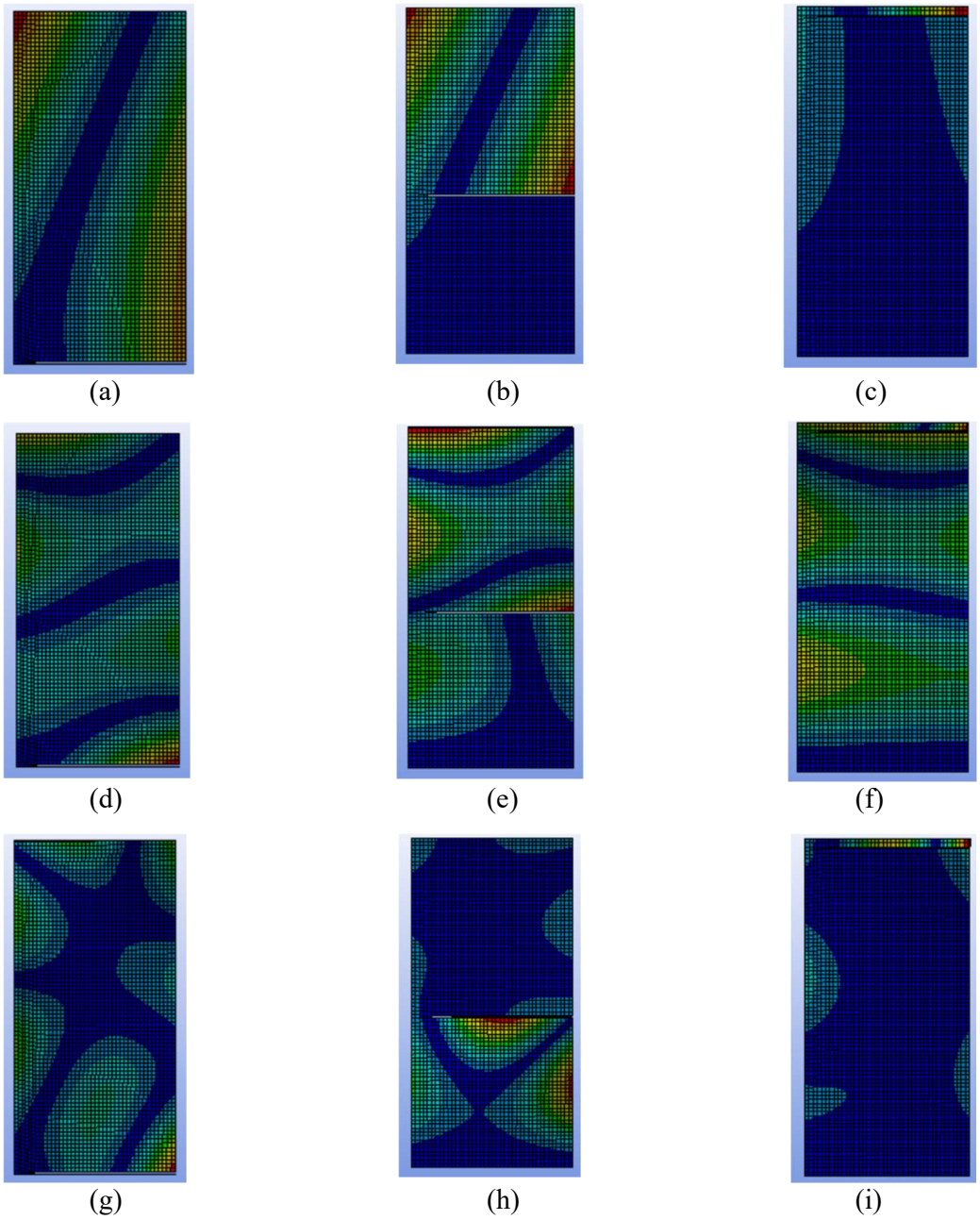

Figure 24: Mode shapes of 2nd [(a), (b) & (c)], 6th [(d), (e) & (f)] & 9th [(g), (h) & (i)] mode of crack length 70mm

Cracks vertical with clamped end and along the clamped edge:

41.25mm crack length:

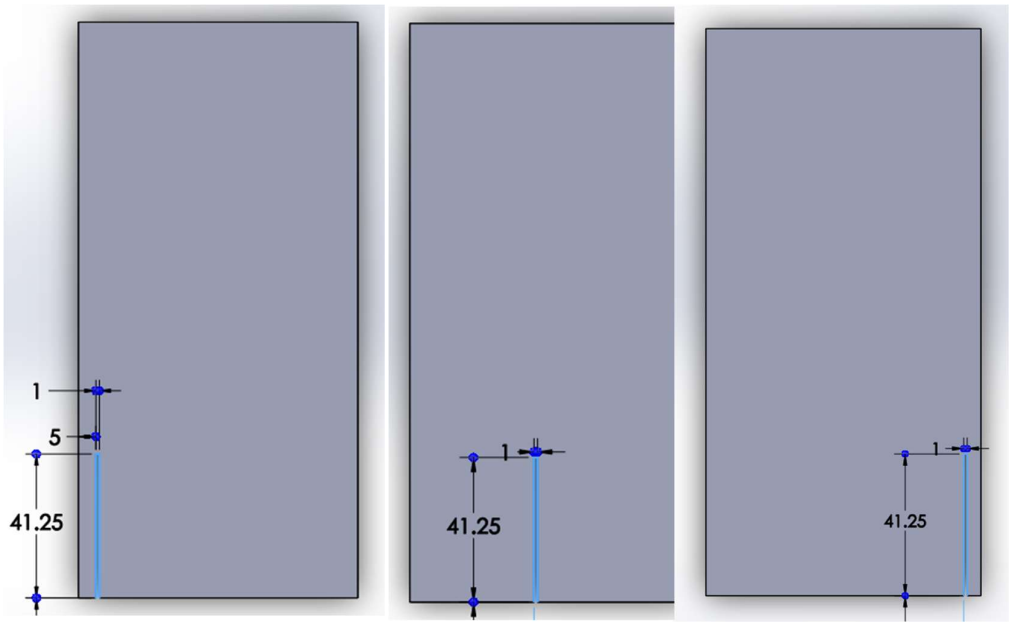

Figure 25: 41.25mm crack length vertical with the clamped end along clamped edge (ACE)

	1	2	3	4	5	6	7	8	9
1	44.123	44.059	43.995	43.936	43.887	43.848	43.821	43.806	43.801
2	191.49	190.98	190.85	190.83	190.87	190.93	190.98	191.02	191.04
3	275.32	275.01	274.81	274.68	274.6	274.57	274.55	274.54	274.54
4	623.97	622.9	622.72	622.75	622.85	622.97	623.07	623.13	623.15
5	773.55	773.05	772.82	772.73	772.72	772.72	772.73	772.74	772.74
6	1197.9	1195.9	1195	1194.6	1194.6	1194.7	1194.9	1195	1195.1
7	1267	1266.2	1265.9	1265.5	1265	1264.4	1263.8	1263.4	1263.3
8	1530.8	1529.8	1528.6	1527	1525.2	1523.1	1521.2	1519.9	1519.5
9	1695.5	1689.6	1686.2	1682.8	1678.7	1673.8	1669.2	1666	1665
10	1975.2	1969.2	1965.3	1963	1961.9	1961.6	1961.6	1961.7	1961.7
11	2361	2344	2329.5	2317.7	2307.3	2298.2	2291	2286.4	2285.1
12	2554.7	2549.2	2546.9	2546.6	2547.4	2548.8	2550.1	2551.1	2551.4
13	2974.4	2960	2948.7	2942	2937.6	2934	2931.3	2929.6	2929.1
14	3259.8	3181	3133.3	3120.9	3126.2	3139.3	3153.9	3165.1	3168.7

(a)

	10	11	12	13	14	15	16	17
1	44.123	44.059	43.995	43.936	43.887	43.848	43.821	43.806
2	191.49	190.98	190.85	190.83	190.87	190.93	190.98	191.02
3	275.32	275.01	274.81	274.68	274.6	274.57	274.55	274.54
4	623.97	622.9	622.72	622.75	622.85	622.97	623.07	623.13
5	773.55	773.05	772.82	772.73	772.72	772.72	772.73	772.74
6	1197.9	1195.9	1195	1194.6	1194.6	1194.7	1194.9	1195
7	1267	1266.2	1265.9	1265.5	1265	1264.4	1263.8	1263.4
8	1530.8	1529.8	1528.6	1527	1525.2	1523.1	1521.2	1519.9
9	1695.5	1689.6	1686.2	1682.8	1678.7	1673.8	1669.2	1666
10	1975.2	1969.2	1965.3	1963	1961.9	1961.6	1961.6	1961.7
11	2361	2344	2329.5	2317.7	2307.3	2298.2	2291	2286.4
12	2554.7	2549.2	2546.9	2546.6	2547.4	2548.8	2550.1	2551.1
13	2974.4	2960	2948.7	2942	2937.6	2934	2931.3	2929.6
14	3259.8	3181	3133.3	3120.9	3126.2	3139.3	3153.9	3165.1

(b)

Table 6: Modal analysis of variation in crack position of 41.25mm crack length vertical with the clamped end ACE (a) & (b)

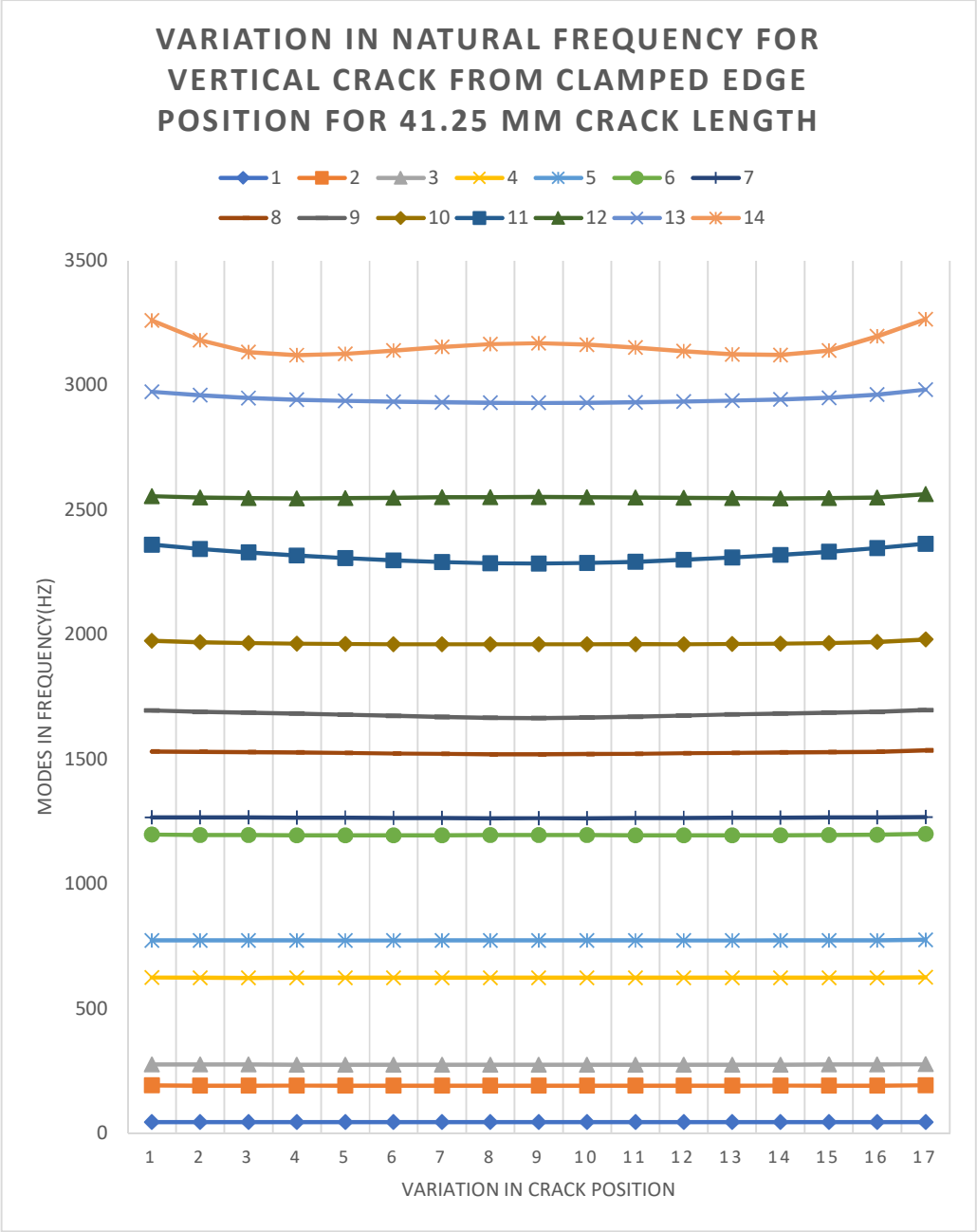

Figure 26: Modal analysis of variation in crack position of 41.25mm crack length vertical with the clamped end ACE

Among these variants of cracks which are placed vertically with the clamped edge, the tables (a) & (b) are of one entire table set among which the rows indicate the mode numbers in frequency consecutively and columns indicate the variation in crack's position from one side of the crack to the other side progressing along the clamped or free end.

The data in this table is of the flat plate with a 41.25 mm crack length vertically positioned along the clamp and progressing along the clamp's one side to the other. From this data's graph the lines of modes are seen to be very streamlined showing almost negligible variation in frequency.

The mode shapes are very much similar to that of the uncracked flat plate. As the crack is very small and position along the clamped edge, it's effects in the mode shapes are almost none. Although in many cases where the crack's position that almost divides the flat into two parts, these parts show distinct behavior in mode shapes. this characteristics is similar to that of the horizontal crack's partitioning the flat plate's mode shapes into distinct parts.

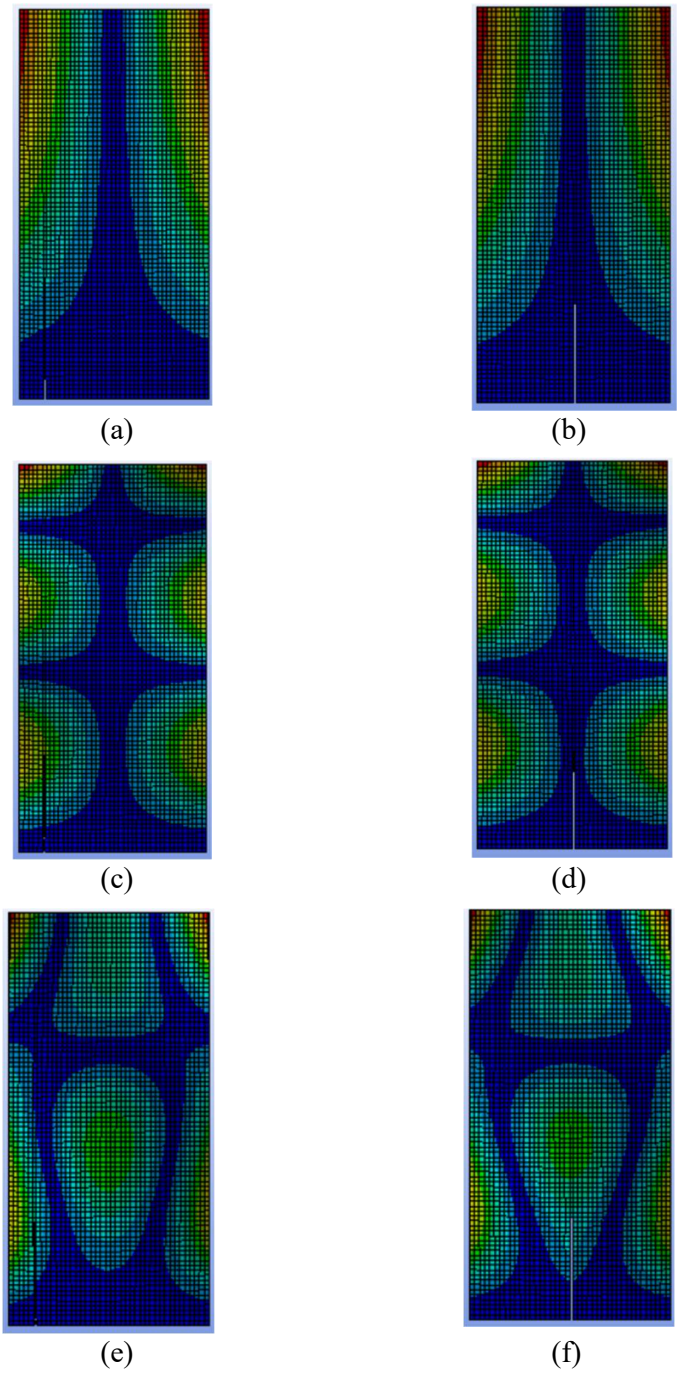

Figure 27: Mode shapes of 2nd [(a), (b)], 6th [(c), (d)] & 9th [(e), (f)] mode of crack length 41.25mm

82.5 mm crack length:

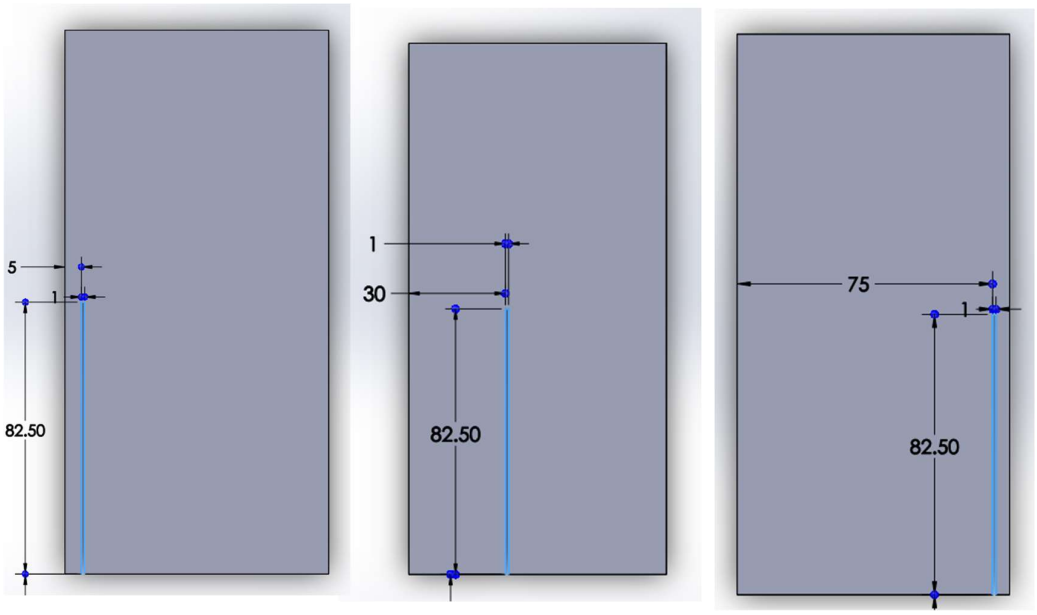

Figure 28: 82.5mm crack length vertical with the clamped end ACE (Along clamped edge)

	1	2	3	4	5	6	7	8	9
1	44.059	43.954	43.857	43.772	43.701	43.646	43.606	43.583	43.576
2	191.43	190.29	189.89	189.61	189.43	189.31	189.23	189.19	189.18
3	275.54	275.18	274.93	274.77	274.66	274.59	274.55	274.53	274.53
4	627.82	620.14	613.28	607.75	603.59	600.65	598.72	597.65	597.35
5	773.87	772.19	770.79	769.54	768.37	767.33	766.51	765.99	765.84
6	1199.7	988.49	966.79	964.65	972.81	987.62	1006.6	1025.9	1034.3
7	1270.5	1205.3	1199.6	1189.6	1175.4	1156.7	1134.4	1112.8	1103.5
8	1533.3	1292.7	1309.7	1324.9	1340.5	1358	1378	1397.1	1404.8
9	1710.7	1535.6	1536.7	1537.6	1538.6	1540	1542.7	1549.8	1564.6
10	1976.7	1790.3	1843.1	1850.5	1822.5	1761.4	1679.7	1607.9	1571.3
11	2366.7	1966.6	1975	2002.4	2020.3	2017.9	2005.8	1996.7	1994.1
12	2554.4	2426.5	2497.5	2524.9	2530.8	2351.4	2249.5	2211.9	2203.5
13	2976.4	2547.4	2559.8	2658.9	2568.3	2535.1	2538.6	2541	2541.8
14	3268.4	2712.7	2678.5	2683.8	2717.9	2737.3	2756.4	2769.2	2773.1

(a)

	10	11	12	13	14	15	16	17
1	43.586	43.613	43.655	43.714	43.788	43.875	43.975	44.059
2	189.2	189.24	189.33	189.46	189.66	189.96	190.4	191.43
3	274.53	274.56	274.6	274.67	274.79	274.97	275.24	275.54
4	597.8	599.03	601.15	604.32	608.74	614.55	621.64	627.82
5	766.06	766.65	767.52	768.59	769.78	771.06	772.5	773.87
6	1022.4	1002.6	984.24	970.56	964.09	969.04	997.41	1199.7
7	1116.7	1139	1160.8	1178.6	1191.9	1201.1	1205.7	1270.5
8	1393.7	1373.9	1354.3	1337.2	1321.9	1306.6	1288.9	1533.3
9	1547.7	1542	1539.7	1538.4	1537.4	1536.5	1535.4	1710.7
10	1620.3	1696.2	1776.2	1830.7	1852.3	1836.1	1775.6	1976.7
11	1998	2008.2	2019.7	2018.4	1996.8	1971.2	1967.7	2366.7
12	2216.5	2263	2385	2529.9	2522.8	2484	2413.6	2554.4
13	2540.7	2538	2534.3	2616.6	2635	2552.8	2548.4	2976.4
14	2767.3	2753	2733.1	2715.3	2681.3	2680.4	2731.7	3268.4

(b)

Table 7: Modal analysis of variation in crack position of 82.5mm crack length vertical with the clamped end ACE (a) & (b)

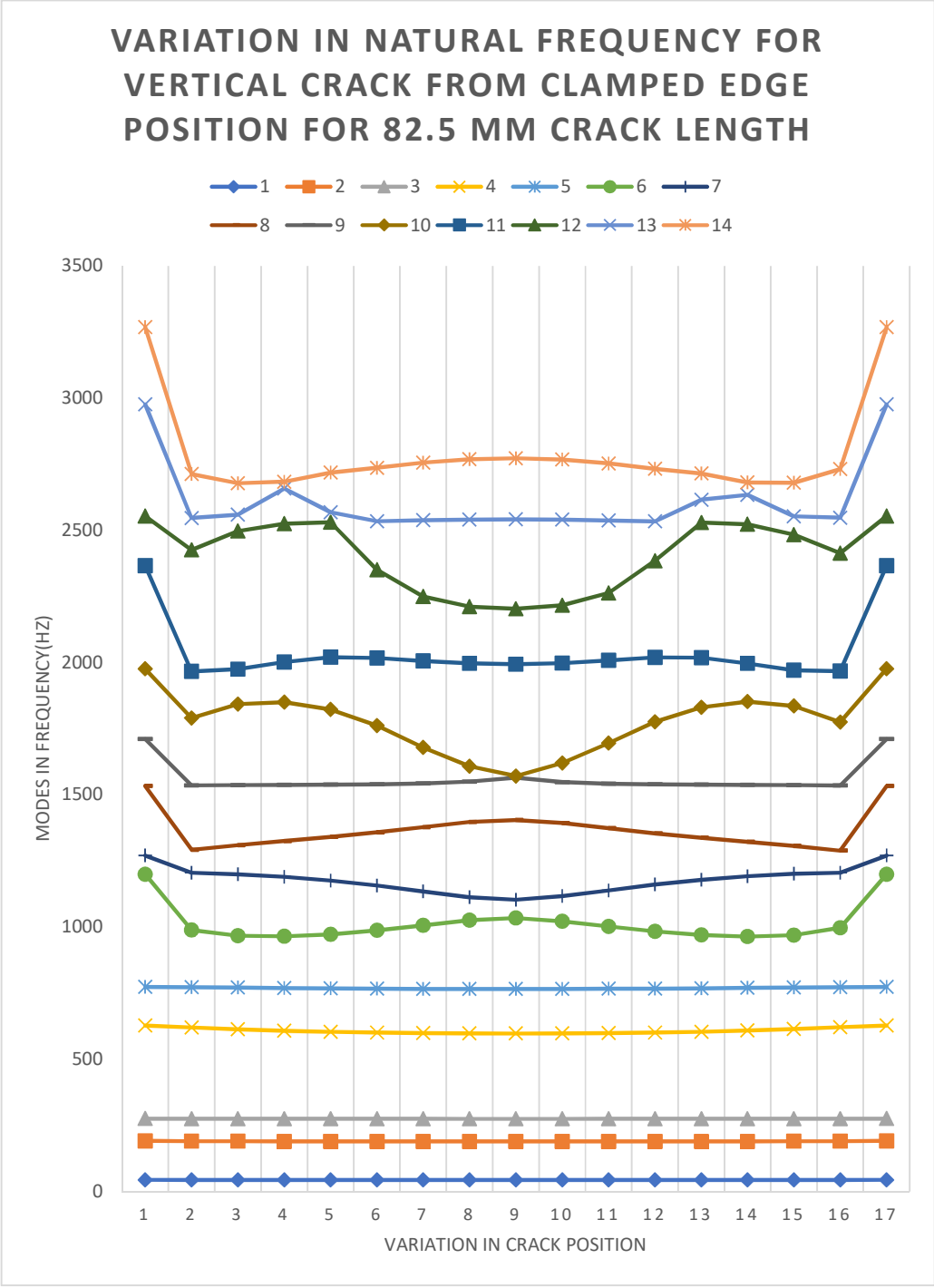

Figure 29: Modal analysis of variation in crack position of 82.5mm crack length vertical with the clamped end ACE

The data in this table is of the flat plate with a 82.5mm crack length vertically positioned along the clamp and progressing along the clamp's one side to the other. This data shows slightly more extreme changes than the previous model of this variant. Although not at all negligible, yet the change is only significant near the edges.

The mode shapes shown for this model shows similar behavorial changes as the previous models.

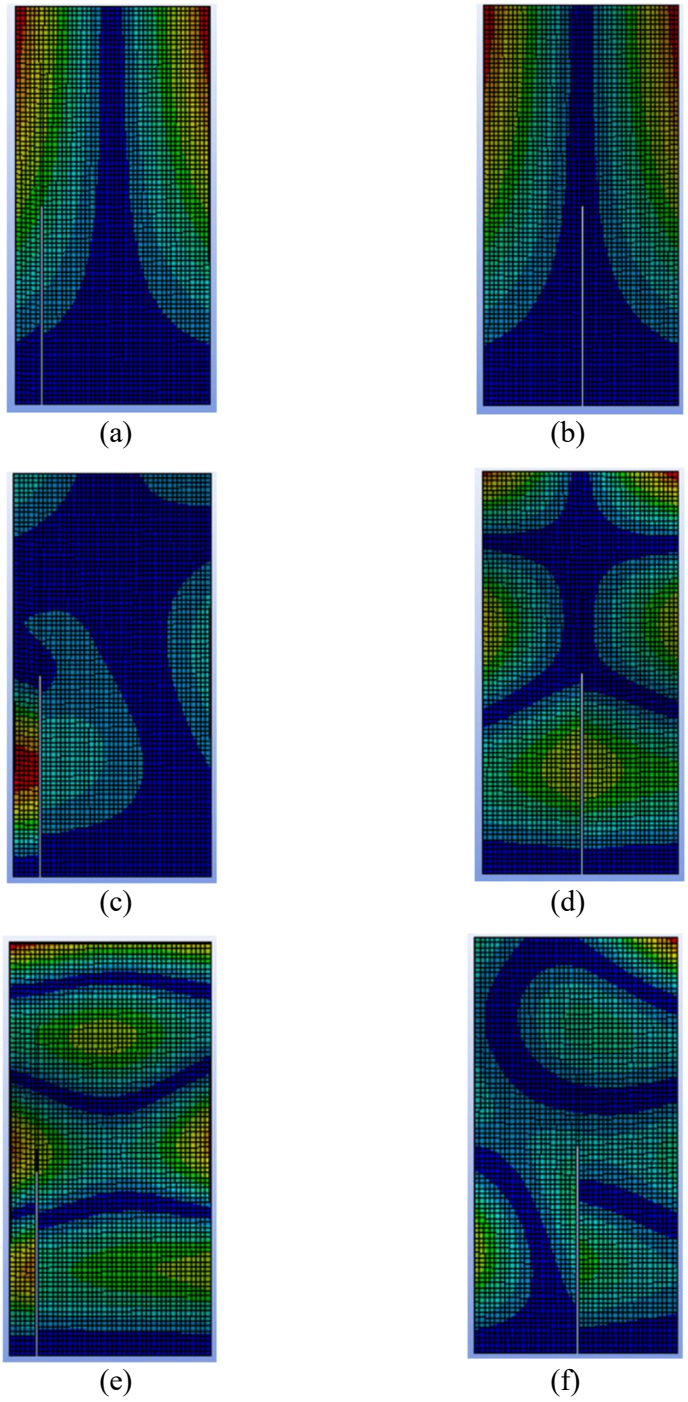

Figure 30: Mode shapes of 2nd [(a), (b)], 6th [(c), (d)] & 9th [(e), (f)] mode of crack length 82.5mm

123.75mm crack length:

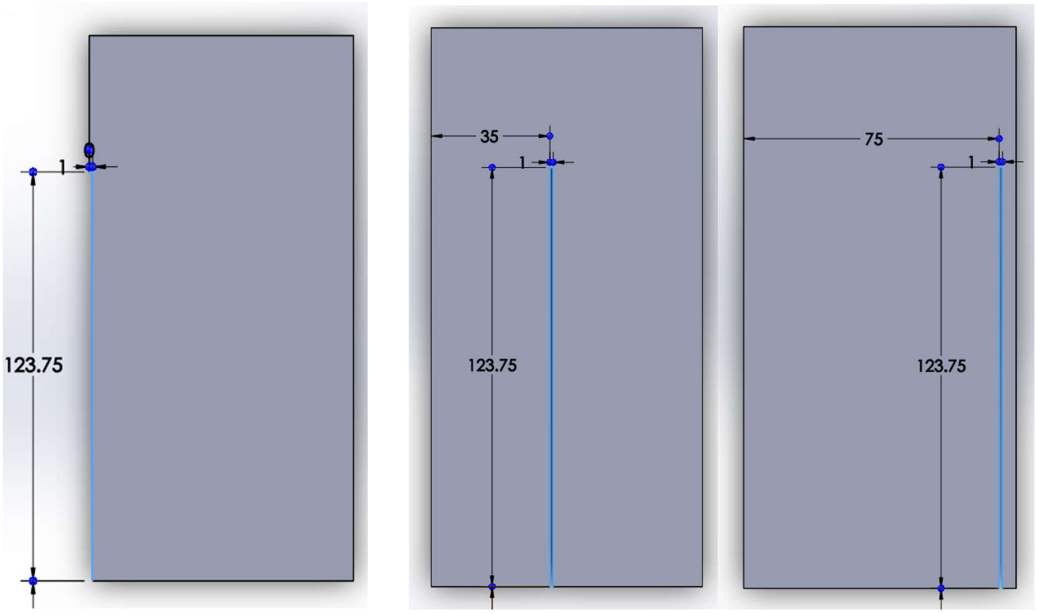

Figure 31: 123.75mm crack length vertical with the clamped end ACE (Along clamped edge)

	1	2	3	4	5	6	7	8	9
1	44.114	43.992	43.885	43.794	43.72	43.663	43.623	43.599	43.592
2	192.36	190.49	189.57	188.84	188.29	187.88	187.62	187.47	187.43
3	275.44	274.86	274.43	274.11	273.88	273.71	273.61	273.55	273.53
4	627.92	452.67	442.36	437.82	436.07	435.73	436.02	436.38	436.51
5	773.82	649.78	668.19	686.39	705.23	724.01	739.21	746.97	748.77
6	1203.1	771.59	770.29	770	771.13	775.04	785.01	801.45	809.89
7	1277.6	1127.7	1085	1057.9	1036.5	1013.7	983.02	948.39	933.62
8	1535.6	1264	1270.5	1266.7	1246.7	1205.5	1156.4	1125.7	1117.7
9	1711.6	1396.4	1441.6	1476.4	1505	1493.2	1423.3	1392.3	1384.9
10	1978	1548.9	1560.3	1568.4	1561.9	1527.8	1541	1547.3	1548.8
11	2383.8	1836.7	1938.8	1917.1	1774.5	1663.6	1664	1678.1	1683.6
12	2552.8	1962.1	2017.3	2208.9	1976.3	1966	1985.2	2021.8	2045.3
13	2975.7	2384.8	2398.8	2270.3	2451.5	2511.9	2492.3	2321.5	2258.4
14	3276.1	2547.7	2540.9	2471.4	2540.4	2554.1	2525.4	2527.7	2528.1

(a)

	10	11	12	13	14	15	16	17
1	43.602	43.629	43.673	43.734	43.811	43.905	44.015	44.114
2	187.49	187.66	187.95	188.38	188.98	189.74	190.71	192.36
3	273.56	273.62	273.74	273.92	274.16	274.5	274.96	275.44
4	436.32	435.94	435.73	436.27	438.44	443.8	456.06	627.92
5	745.99	736.71	720.38	701.41	682.71	664.58	645.88	773.82
6	798.1	782.36	773.91	770.75	769.96	770.47	771.97	1203.1
7	954.71	989.88	1018.7	1040.7	1062.7	1091.8	1139.7	1277.6
8	1129.9	1165.4	1215.2	1252.4	1268.6	1269.9	1262.2	1535.6
9	1396.3	1433.7	1510.7	1499.8	1469.9	1433.6	1385.4	1711.6
10	1546.5	1539	1524.8	1566.1	1567.3	1558.1	1546.4	1978
11	1675.6	1661.6	1671.1	1817.5	1923.9	1939.3	1808	2383.8
12	2013.7	1979.7	1964.8	1990.1	2189.4	1981.1	1965.7	2552.8
13	2349.3	2524.4	2504.7	2426.2	2335.9	2394.6	2385.1	2975.7
14	2527.5	2533	2549.2	2536.8	2478.4	2542.5	2549.1	3276.1

(b)

Table 8: Modal analysis of variation in crack position of 123.75mm crack length vertical with the clamped end ACE (a) & (b)

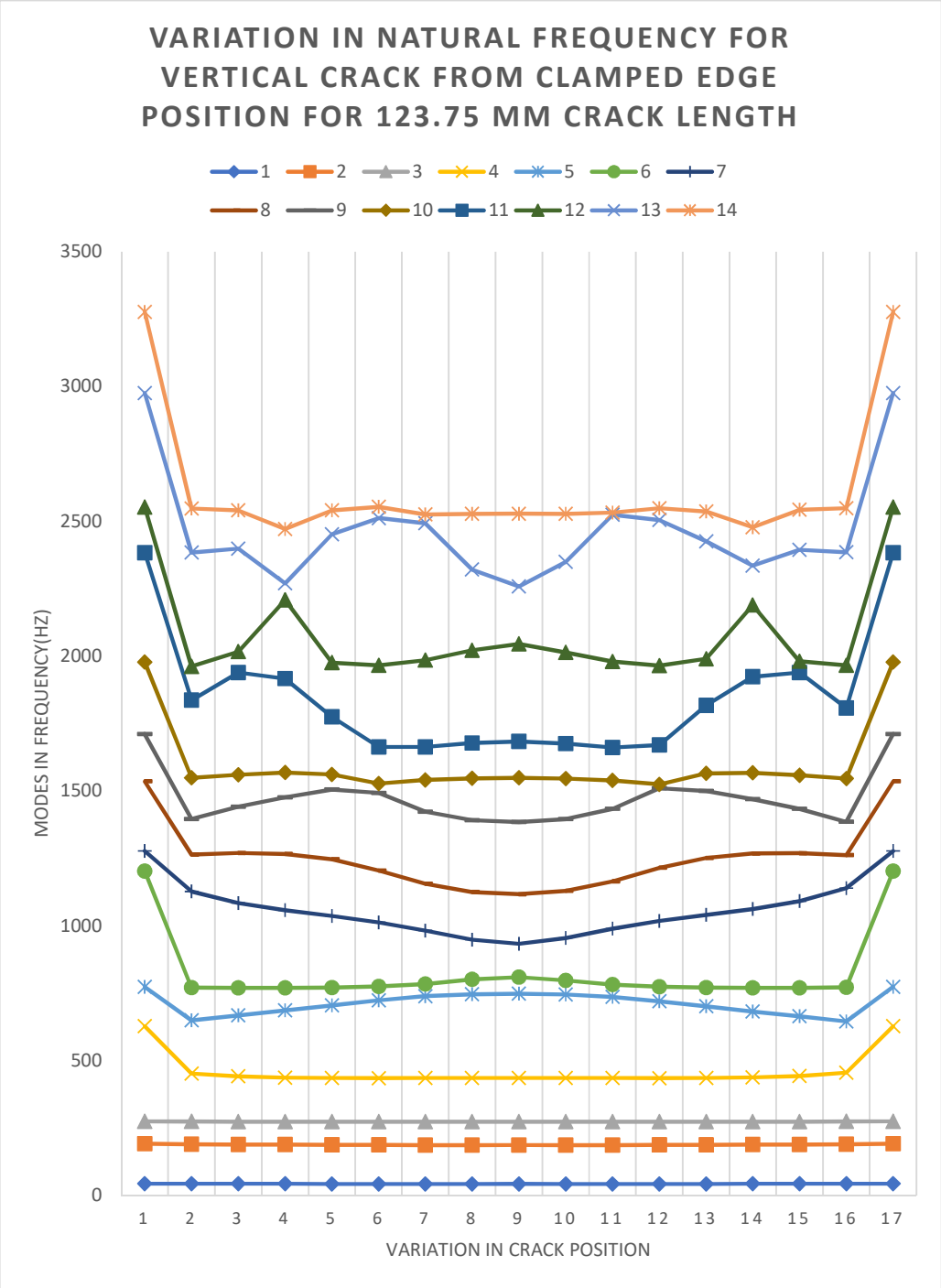

Figure 32: Modal analysis of variation in crack position of 123.75mm crack length vertical with the clamped end ACE

The data in this table is of the flat plate with a 123.75 mm crack length vertically positioned along the clamp and progressing along the clamp's one side to the other. This model shows the most extreme behavior of this specific variant. The extreme points in the specific positions in the graph show similarities with other models.

The mode shapes seen below show more shifting due to longer crack length. The similarites with uncracked flat plate can be clearly seen. The mode shapes seem to show two distict portion of mode shapes that vary upon the change in the crack's position and they somewhat merge at the crack's disappearing position. These behaviors are seen mostly throughout the work.

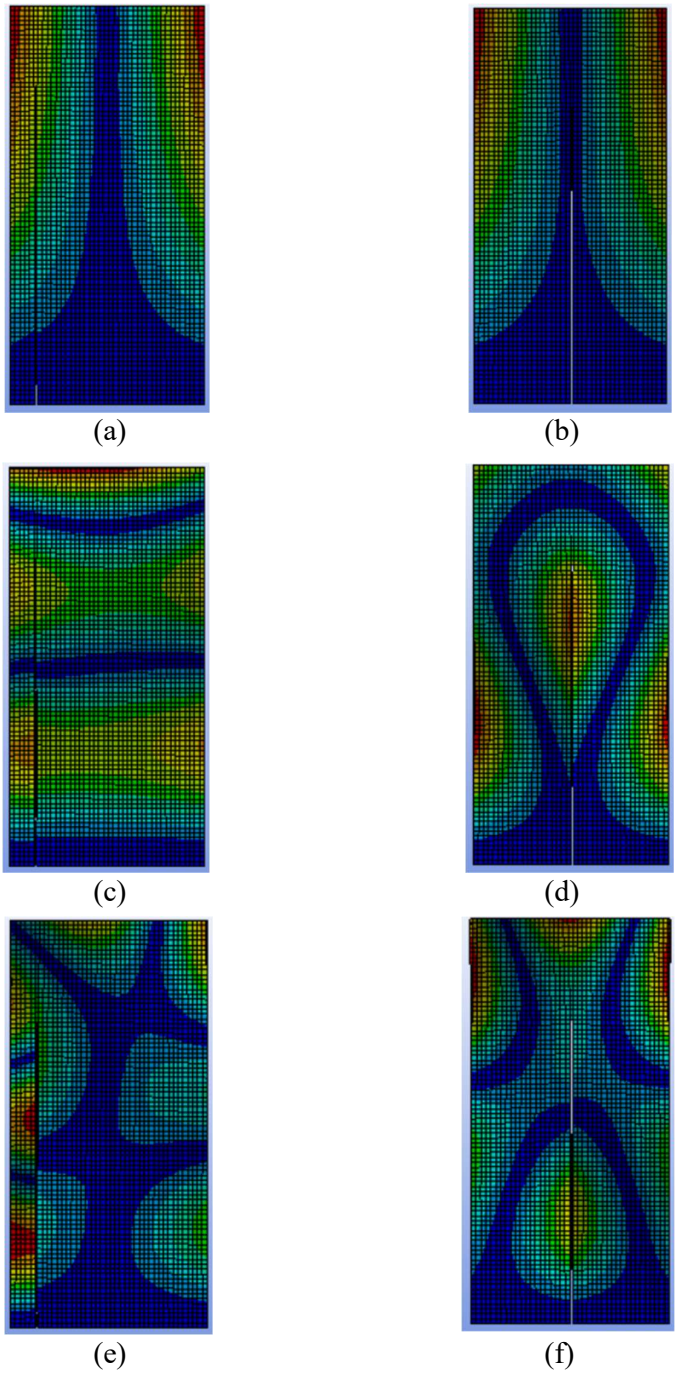

Figure 33: Mode shapes of 2nd [(a), (b)], 6th [(c), (d)] & 9th [(e), (f)] mode of crack length 123.75mm

Cracks vertical with clamped end and along the free edge:

41.25mm crack length:

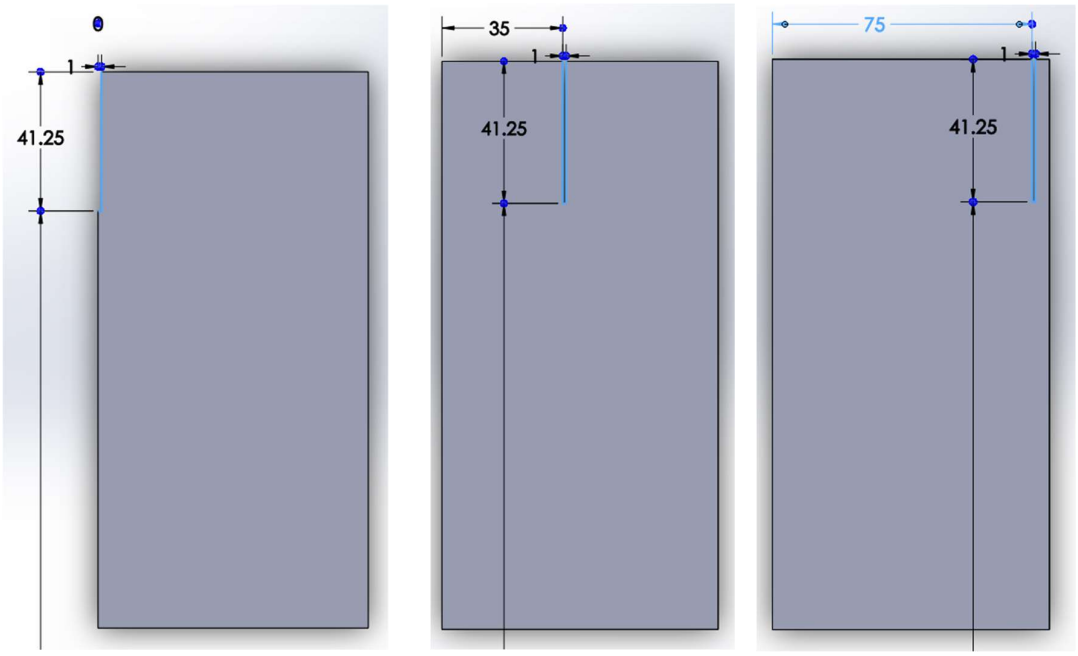

Figure 34: 41.25mm crack length vertical with the clamped end AFE (Along Free edge)

	1	2	3	4	5	6	7	8	9
1	44.51	44.508	44.506	44.503	44.501	44.499	44.498	44.497	44.496
2	194.03	191.48	188.59	185.81	183.37	181.42	180.02	179.19	178.96
3	276.16	276.1	276.04	275.97	275.91	275.85	275.82	275.8	275.79
4	627.93	522.44	483.24	463.85	453.76	448.62	446.21	445.23	445.01
5	774.2	687.3	706.66	724.58	741.26	754.4	761.64	764.6	765.29
6	1200.4	776.25	777.94	780.43	785.23	795.83	815.6	842.58	859.48
7	1284.6	1194.6	1178.7	1151.1	1108.6	1052.8	992.7	939.59	914.92
8	1530.9	1358.5	1407	1434	1446.7	1453.1	1459.4	1466.5	1469.6
9	1705.1	1530.3	1528.8	1527.3	1526.7	1526.8	1526.9	1526.3	1525.7
10	1977.6	1781.2	1861.1	1861.8	1798.3	1712.6	1644.3	1604.3	1592.8
11	2360.9	1964.6	1965.1	2027.5	2050.9	2021.4	1999.1	1988.3	1985.6
12	2554.2	2365.8	2358.2	2347.8	2329.5	2313.8	2306.1	2302.2	2301.1
13	2980.2	2556.2	2562.2	2568	2529.1	2519.6	2523	2525.8	2526.6
14	3261.5	2922.7	2831.7	2736	2757.9	2852.7	2855.7	2856.8	2857.1

(a)

	10	11	12	13	14	15	16	17
1	44.497	44.498	44.499	44.502	44.504	44.506	44.509	44.51
2	179.31	180.25	181.77	183.82	186.34	189.17	192.04	194.03
3	275.8	275.82	275.86	275.92	275.98	276.05	276.12	276.16
4	445.35	446.54	449.38	455.28	466.79	488.92	535.02	627.93
5	764.23	760.62	752.22	738.1	721.07	702.94	683.1	774.2
6	836.93	810.93	793.03	783.95	779.82	777.57	775.94	1200.4
7	949.08	1004.5	1064.7	1118.4	1157.8	1182.6	1196.7	1284.6
8	1465.2	1458	1452	1444.9	1430	1399.3	1345.8	1530.9
9	1526.4	1526.9	1526.7	1526.7	1527.5	1529.1	1530.5	1705.1
10	1610	1655.7	1729.3	1814.2	1868.6	1848.4	1764.4	1977.6
11	1989.8	2002.5	2027.5	2053.2	2013.4	1961	1967.2	2360.9
12	2302.8	2307.3	2316.1	2333.8	2350.1	2360.1	2366.3	2554.2
13	2525.4	2522.3	2519.4	2536.6	2568.8	2560.5	2555.6	2980.2
14	2856.6	2855.4	2849.2	2734.7	2755.9	2849.1	2939.7	3261.5

(b)

Table 9: Modal analysis of variation in crack position of 41.25mm crack length vertical with the clamped end AFE (a) & (b)

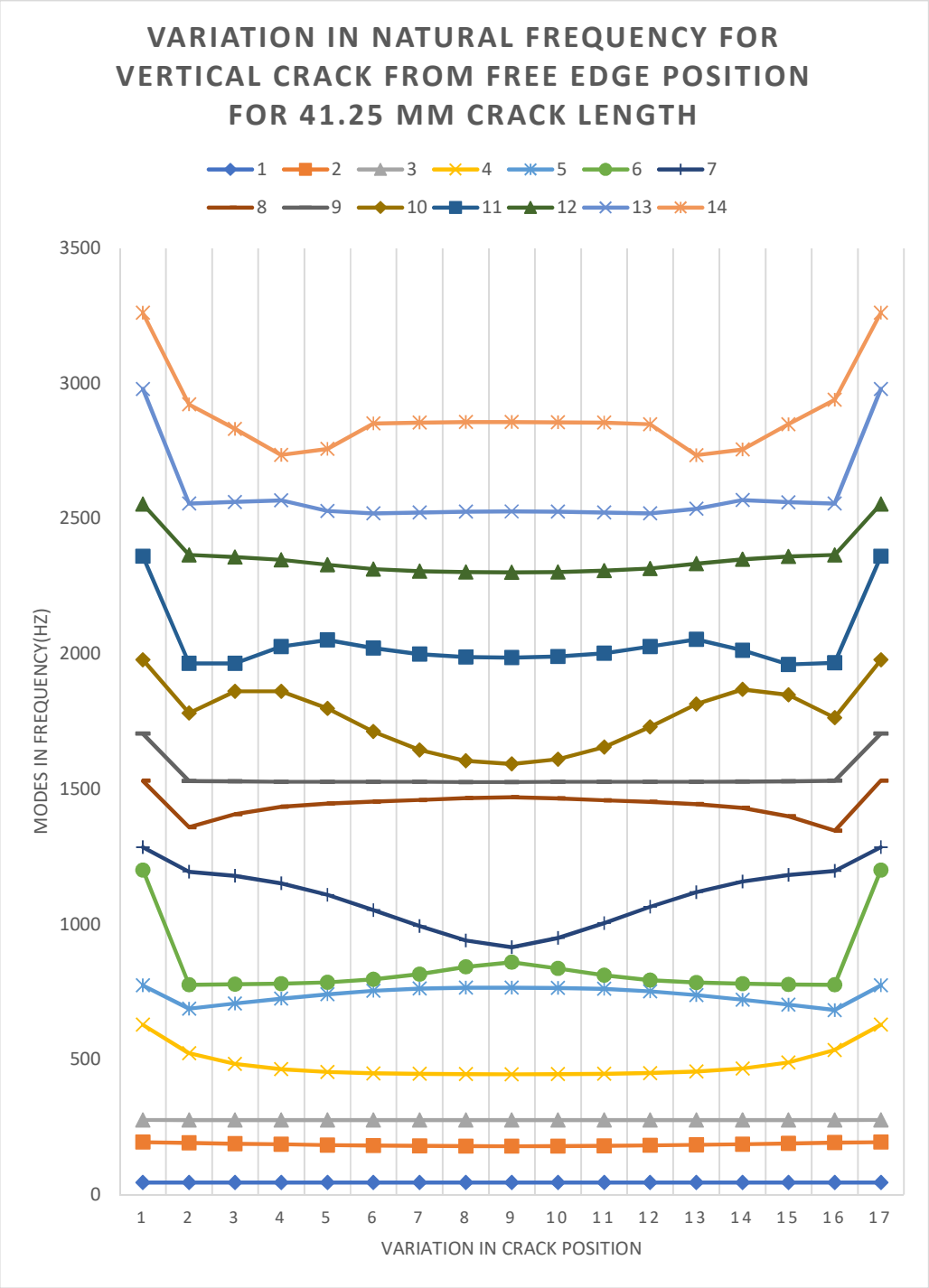

Figure 35: Modal analysis of variation in crack position of 41.25mm crack length vertical with the clamped end AFE

The data in this table is of the flat plate with a 41.25mm crack length positioned vertically with the clamp and progressing along the free end's one side to the other. These set of data plotted graphically shows symmetrical lines for each mode along crack position variation. In each line the first and last data are seen higher than any other data. This is because the models made for this type of crack included crack at the very edge, which basically is a reduced form of the flat plate without a crack and thus has a lower mass in total which increases the modal frequencies at those points. In practical approach, the variations exist in between one side to the middle which is the 9^{th} position for the crack in the table. For this model the variations seen are so small that it might be in many cases negligible.

The 2^{nd}, 6^{th} and 9^{th} mode shapes are taken for the variations of 3^{rd} position of the crack and the 9^{th} position of the crack. These mode shapes also show the shifting of mode shapes from the uncracked flat plate's mode shapes along the variation in crack's position.

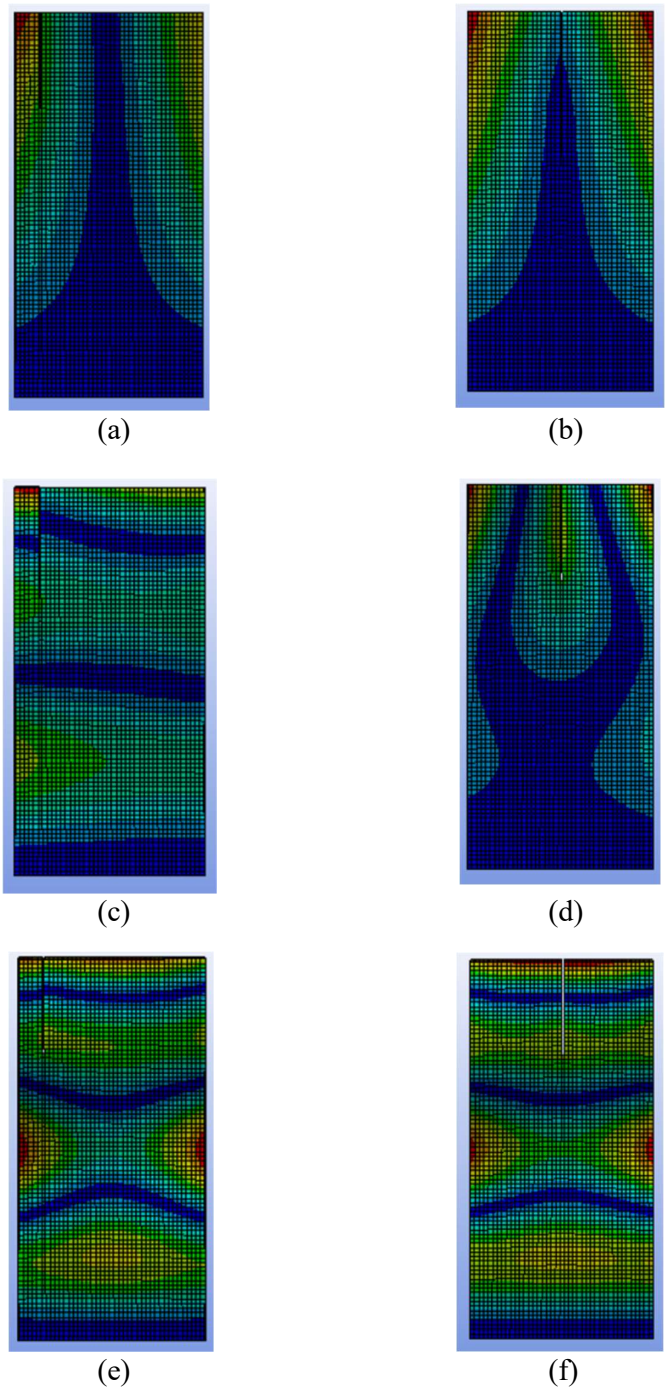

Figure 36: Mode shapes of 2nd [(a), (b)], 6th [(c), (d)] & 9th [(e), (f)] mode of crack length 41.25mm

82.5mm crack length:

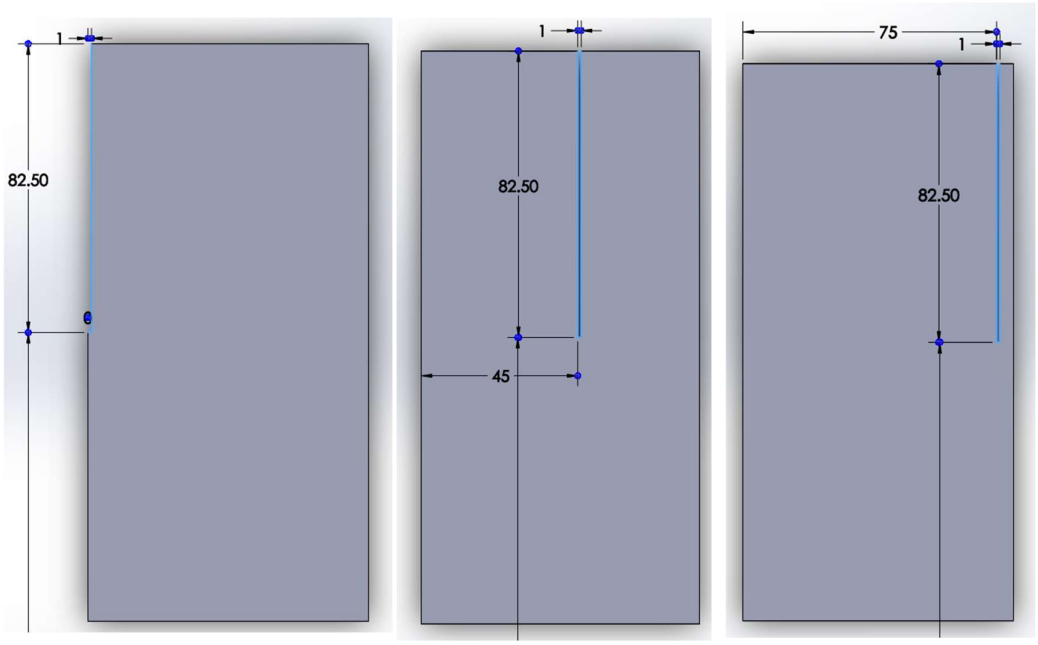

Figure 37: 82.5mm crack length vertical with the clamped end AFE (Along Free edge)

1	44.561	44.555	44.548	44.542	44.537	44.533	44.53	44.528	44.528
2	194.98	139.72	127.65	120.23	115.27	111.92	109.75	108.55	108.21
3	275.98	223.38	242.36	259.67	273.7	275.23	275.35	275.37	275.37
4	627.94	275.97	275.97	276.1	278.97	293.65	307.99	318.35	321.7
5	774.31	621.81	610.85	597.61	582.93	566.82	550.19	536.8	532.24
6	1203.7	773.94	773.41	772.78	772.12	771.53	771.18	771.38	772.15
7	1292.5	944.41	911.65	901.47	900.71	902.37	842.69	795.76	782.64
8	1532.9	1255.4	1281.2	1259.2	1091	938.6	909.28	911.79	912.65
9	1705.2	1423.3	1502.4	1462.8	1413.1	1432.7	1459.7	1480.7	1487.6
10	1978.9	1534.6	1541	1517.1	1519.6	1520.5	1521.2	1522	1522.5
11	2378.3	1764.5	1862.5	1773.9	1716.5	1700.1	1685.2	1672.7	1668.2
12	2552.6	1970.4	1960	1979.5	1993.7	2021.2	2063.6	2120.6	2156.2
13	2980	2444.8	2307.7	2087.6	2345	2500.3	2508.7	2401.2	2333
14	3269.5	2554.5	2497.3	2514.5	2530.8	2587	2568.7	2518	2517.5

(a)

	10	11	12	13	14	15	16	17
1	44.528	44.53	44.534	44.538	44.543	44.55	44.557	44.561
2	108.72	110.1	112.48	116.12	121.48	129.57	143.21	194.98
3	275.37	275.33	275.16	271.94	256.29	238.75	219.13	275.98
4	316.75	305.34	290.57	277.39	276.05	275.96	275.98	627.94
5	538.94	553.43	570.14	585.98	600.38	613.27	623.55	774.31
6	771.27	771.22	771.64	772.25	772.91	773.52	774.03	1203.7
7	802.23	856.84	902.41	900.45	902.5	915.71	956.45	1292.5
8	911.38	908.82	963.31	1128.7	1273.7	1277.6	1248.3	1532.9
9	1477.4	1454.4	1427.5	1413	1489.5	1493.6	1399.3	1705.2
10	1521.8	1521	1520.3	1519.3	1516	1540.5	1534	1978.9
11	1674.7	1688.1	1703.1	1721.4	1808.4	1839	1750.6	2378.3
12	2108.5	2053.8	2014.6	1989.8	1976.9	1962.6	1972.4	2552.6
13	2428.9	2509.6	2491.4	2289.8	2051.8	2437.5	2434.1	2980
14	2518.5	2593.7	2572.7	2527	2510.8	2511.4	2554.5	3269.5

(b)

Table 10: Modal analysis of variation in crack position of 82.5mm crack length vertical with the clamped end AFE (a) & (b)

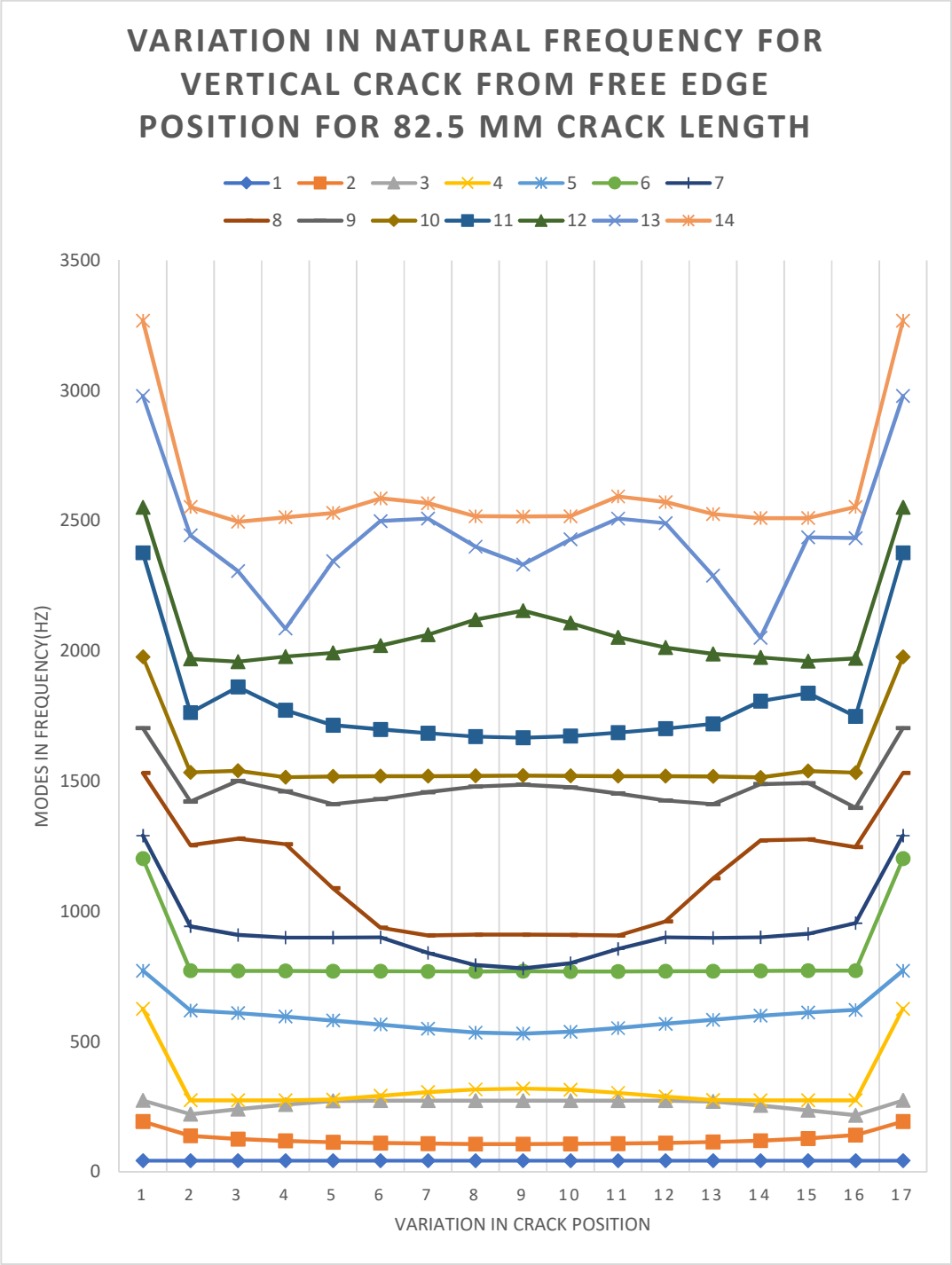

Figure 38: Modal analysis of variation in crack position of 82.5mm crack length vertical with the clamped end AFE

The data in this table is of the flat plate with a 82.5 mm crack length positioned vertically with the clamp and progressing along the free end's one side to the other. These data set when put onto a graph shows more extreme changes with regard to the previous model of vertical type cracks.

The mode shapes of this model shifts it's shapes in accordance with the length and position of the crack. The deformity of the plate from the uncracked one changes the mode shapes and modal frequencies according to crack variants.

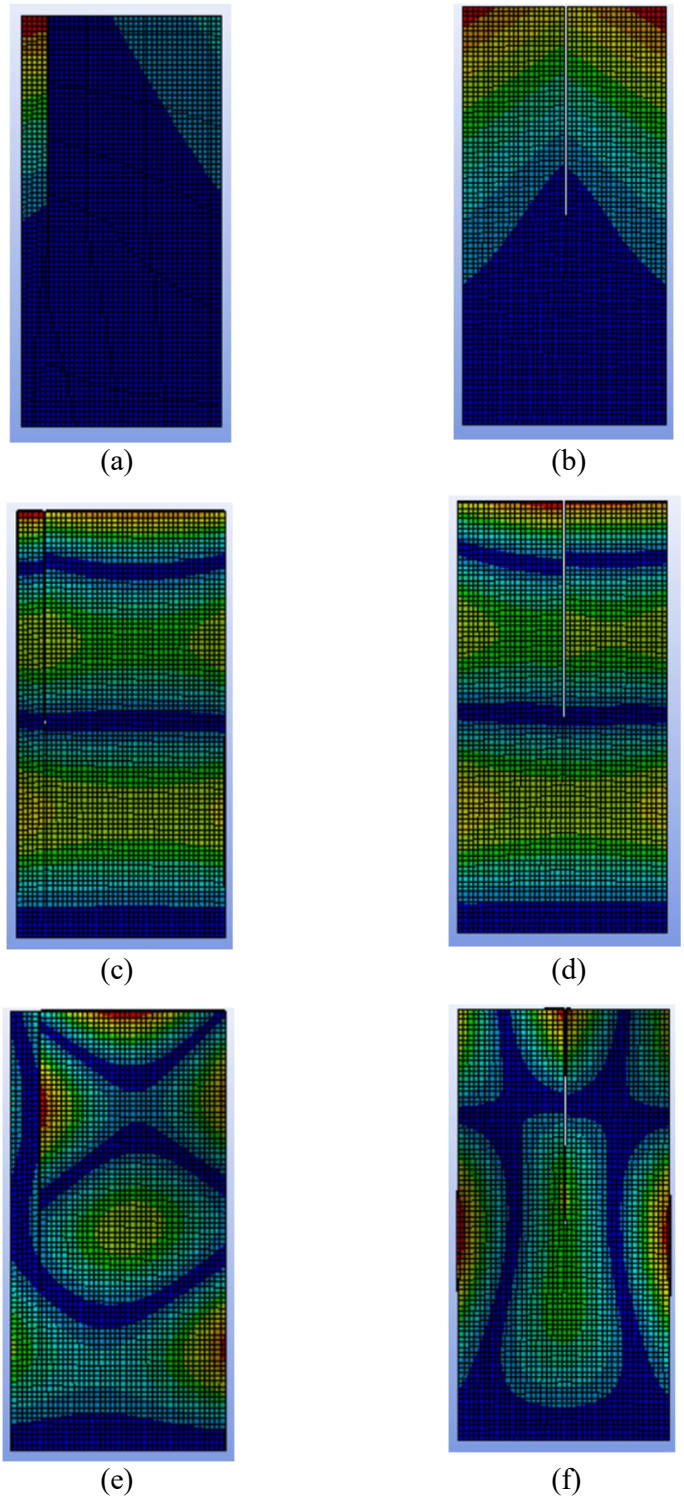

Figure 39: Mode shapes of 2nd [(a), (b)], 6th [(c), (d)] & 9th [(e), (f)] mode of crack length 82.5mm

123.75mm crack length:

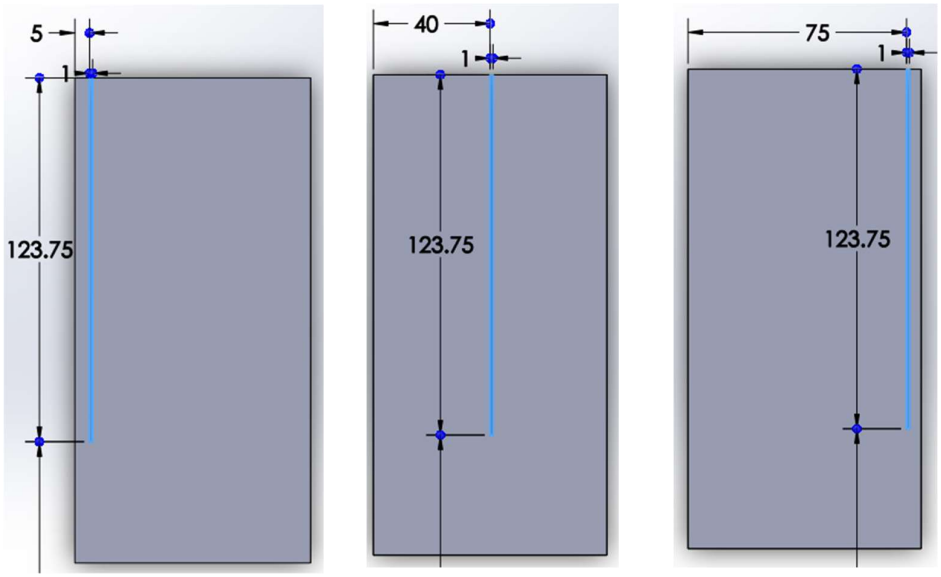

Figure 40: 123.75mm crack length vertical with the clamped end AFE (Along Free edge)

	1	2	3	4	5	6	7	8	9
1	44.489	44.481	44.473	44.465	44.457	44.45	44.444	44.441	44.44
2	194.92	69.273	65.819	63.502	61.881	60.755	60.016	59.604	59.489
3	276.27	209.76	224.88	240.91	258.19	275.07	274.96	274.9	274.88
4	631.92	275.98	275.7	275.44	275.23	276.6	294.94	309.41	314.27
5	774.52	428.05	405.9	392.22	383.7	379.38	379.8	386.51	392.56
6	1205.8	678.01	717.4	753.89	748.72	624.56	533.74	475	453.93
7	1295.9	773.84	772.93	771.9	773.11	771.5	771	770.75	770.69
8	1535.7	1128.2	1074.4	972.14	813.65	832.57	857.55	872.93	877.29
9	1720.2	1332.2	1383.3	1149.2	1094.4	1098.1	1125.9	1172.1	1200.4
10	1980.7	1453.4	1498.6	1437.1	1490.4	1513.2	1504.1	1416.6	1367.3
11	2383.6	1564.7	1552	1513.9	1514.3	1535.9	1531.1	1517.3	1516.6
12	2552.2	1823.7	1715.9	1859.6	1825.7	1743.2	1661.9	1666.3	1673.5
13	2982.2	2008.3	1916.3	1981.8	2286	2180.9	2085.6	2066.8	2066.9
14	3277.5	2371.8	2114	2249.9	2335.4	2478.8	2503.9	2503.9	2497.3

(a)

	10	11	12	13	14	15	16	17
1	44.442	44.445	44.451	44.459	44.466	44.475	44.483	44.489
2	59.662	60.136	60.947	62.161	63.901	66.395	70.192	194.92
3	274.91	274.98	272.86	254.63	237.61	221.79	206.8	276.27
4	307.11	291.41	275.1	275.27	275.49	275.75	276.04	631.92
5	384.68	379.26	379.91	385.06	394.48	409.47	434.24	774.52
6	484.3	549.13	647.32	763.59	746.98	709.74	669.66	1205.8
7	770.79	771.07	771.66	773.74	772.12	773.12	774	1295.9
8	870.73	853.21	826.93	826.82	1006.2	1084.7	1141.5	1535.7
9	1162.2	1118.6	1095.3	1097.6	1187.9	1373	1322.4	1720.2
10	1436.2	1508.9	1513.5	1480	1426.4	1501.1	1428.5	1980.7
11	1517.9	1539.2	1528.5	1514.3	1513.6	1659.3	1553.9	2383.6
12	1663.4	1669.9	1763.7	1836	1855.9	1692.6	1809.9	2552.2
13	2067.7	2096	2215.8	2219.8	1936.7	1942.7	1998.4	2982.2
14	2504.4	2503.2	2465.6	2328.7	2224.4	2087.4	2374.7	3277.5

(b)

Table 11: Modal analysis of variation in crack position of 123.75mm crack length vertical with the clamped end AFE (a) & (b)

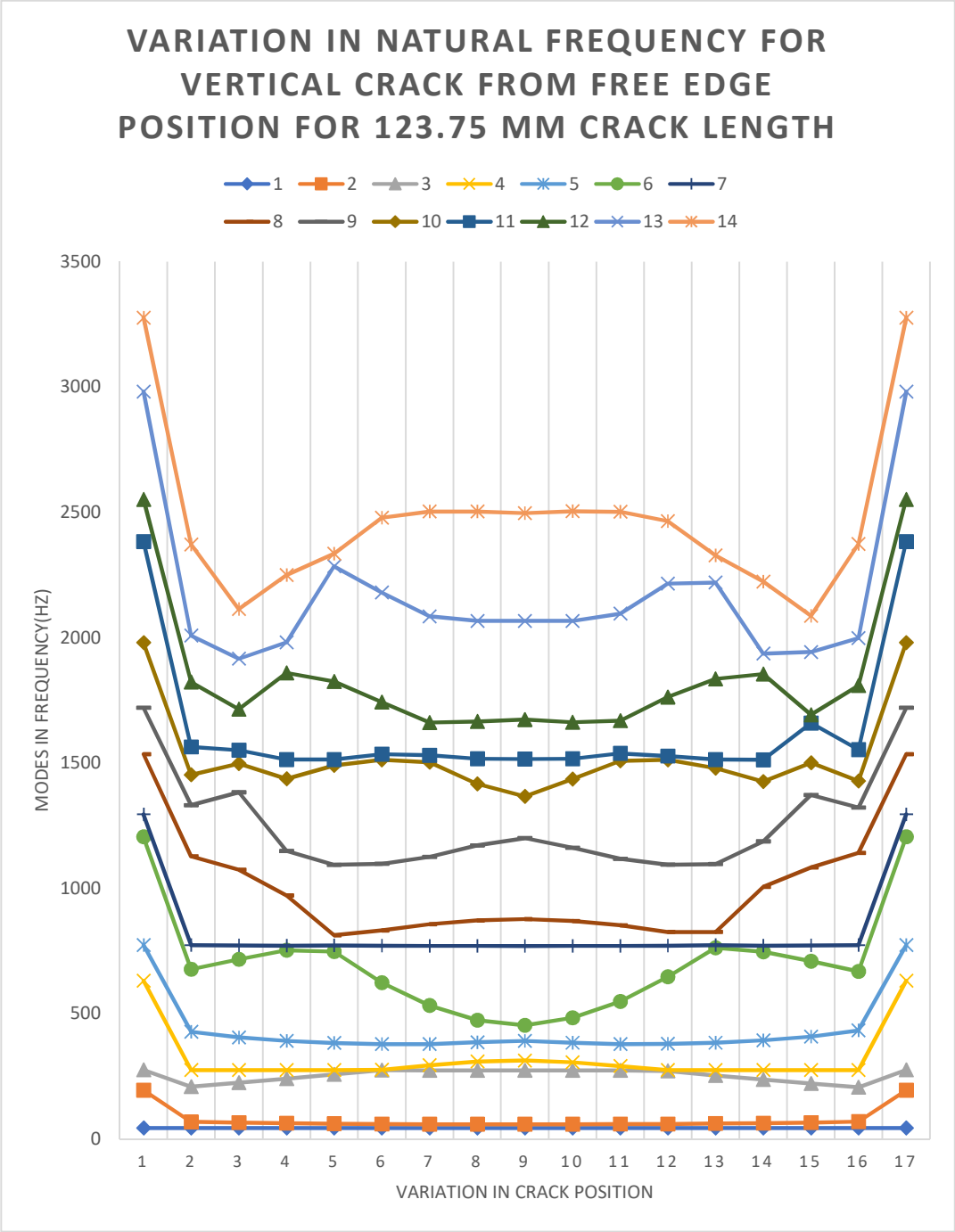

Figure 41: Modal analysis of variation in crack position of 123.75mm crack length vertical with the clamped end AFE

The data in this table is of the flat plate with a 123.75 mm crack length positioned vertically with the clamp and progressing along the free end's one side to the other. This data set put graphically shows the most extreme behavior among the three models of this variant. The extreme points are much sharper in the mode lines in this model in contrast with the other models.

The mode shapes of this model are as seen below:

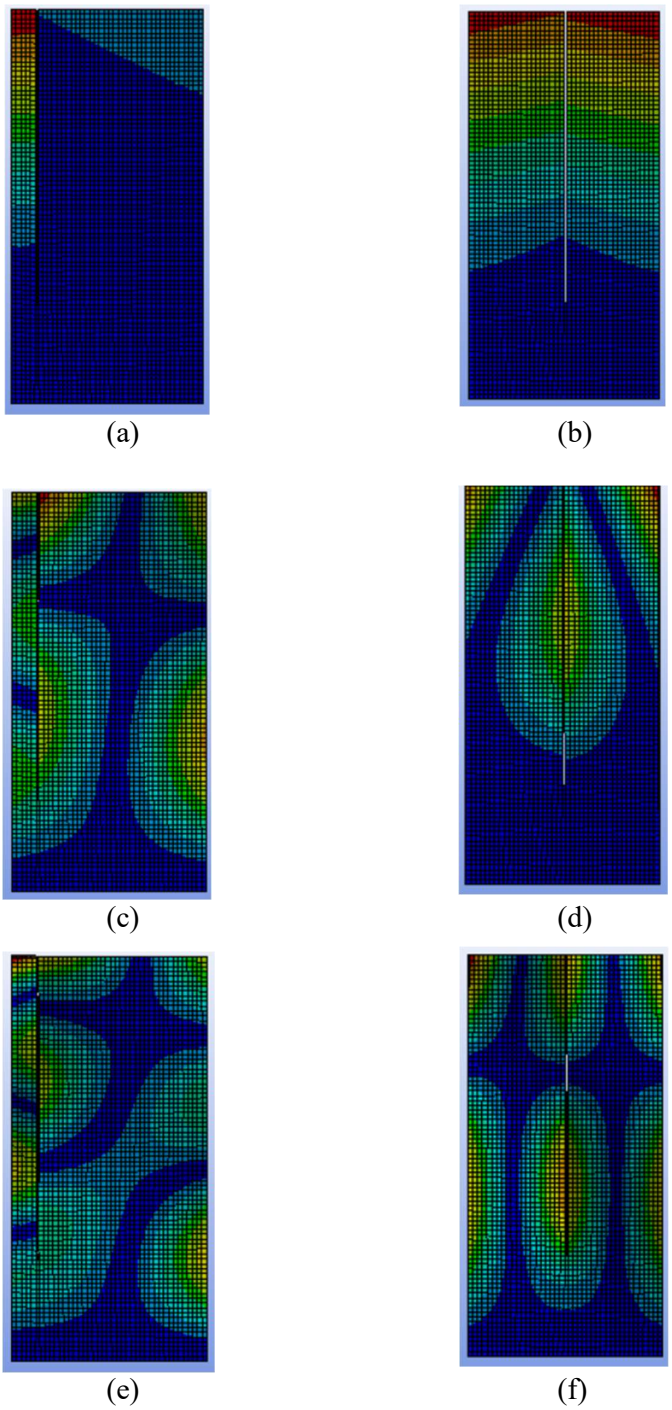

Figure 42: Mode shapes of 2nd [(a), (b)], 6th [(c), (d)] & 9th [(e), (f)] mode of crack length 123.75mm

Comparison with the output of flat plate:

The deviation in output are seen more with longer crack length. So, only the modes of 70mm horizontal crack and 123.75mm vertical crack of both types are shown in comparison with the flat plate.

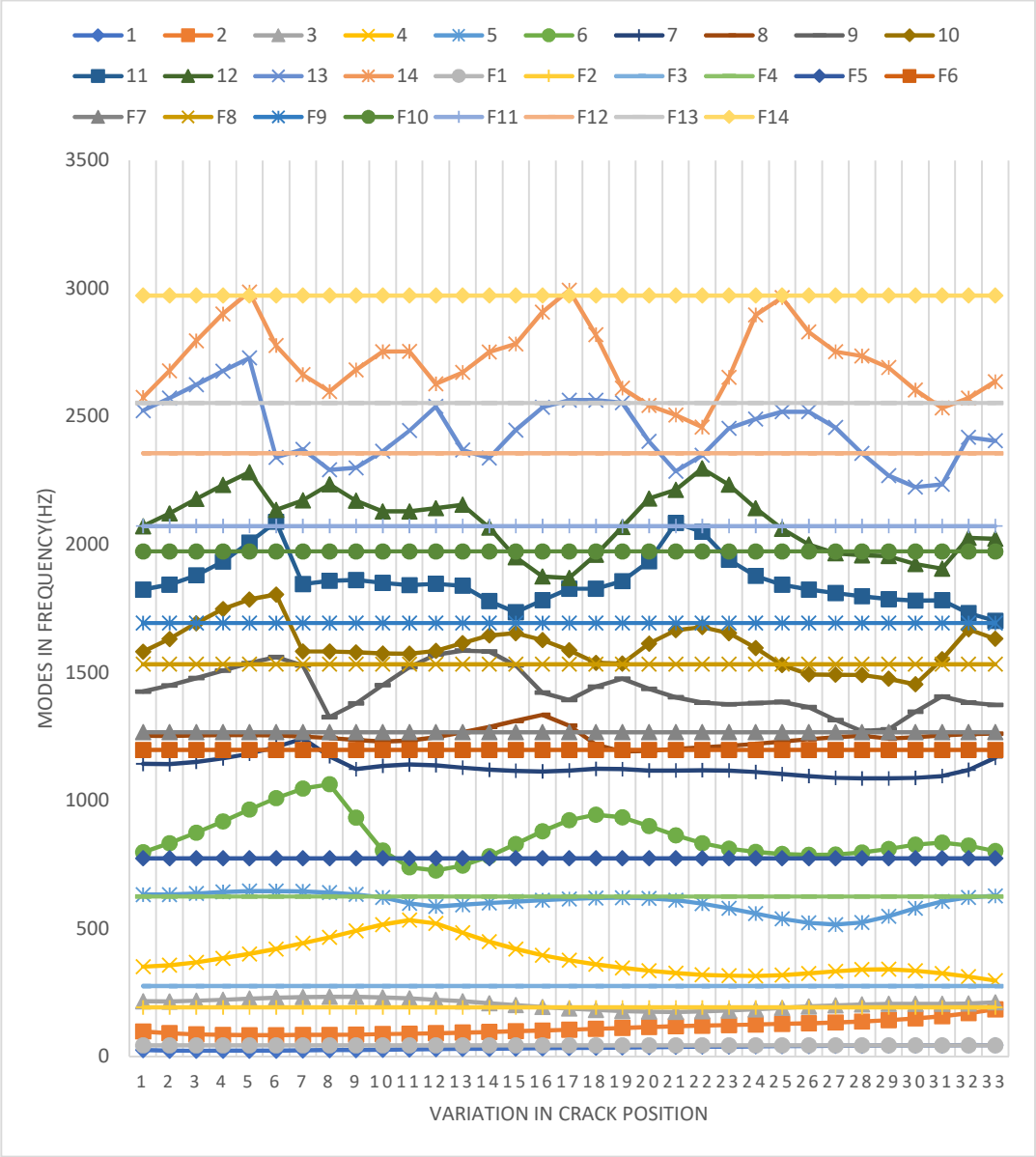

Figure 43: Mode Comparison of 70mm Horizontal Crack length with flat plate

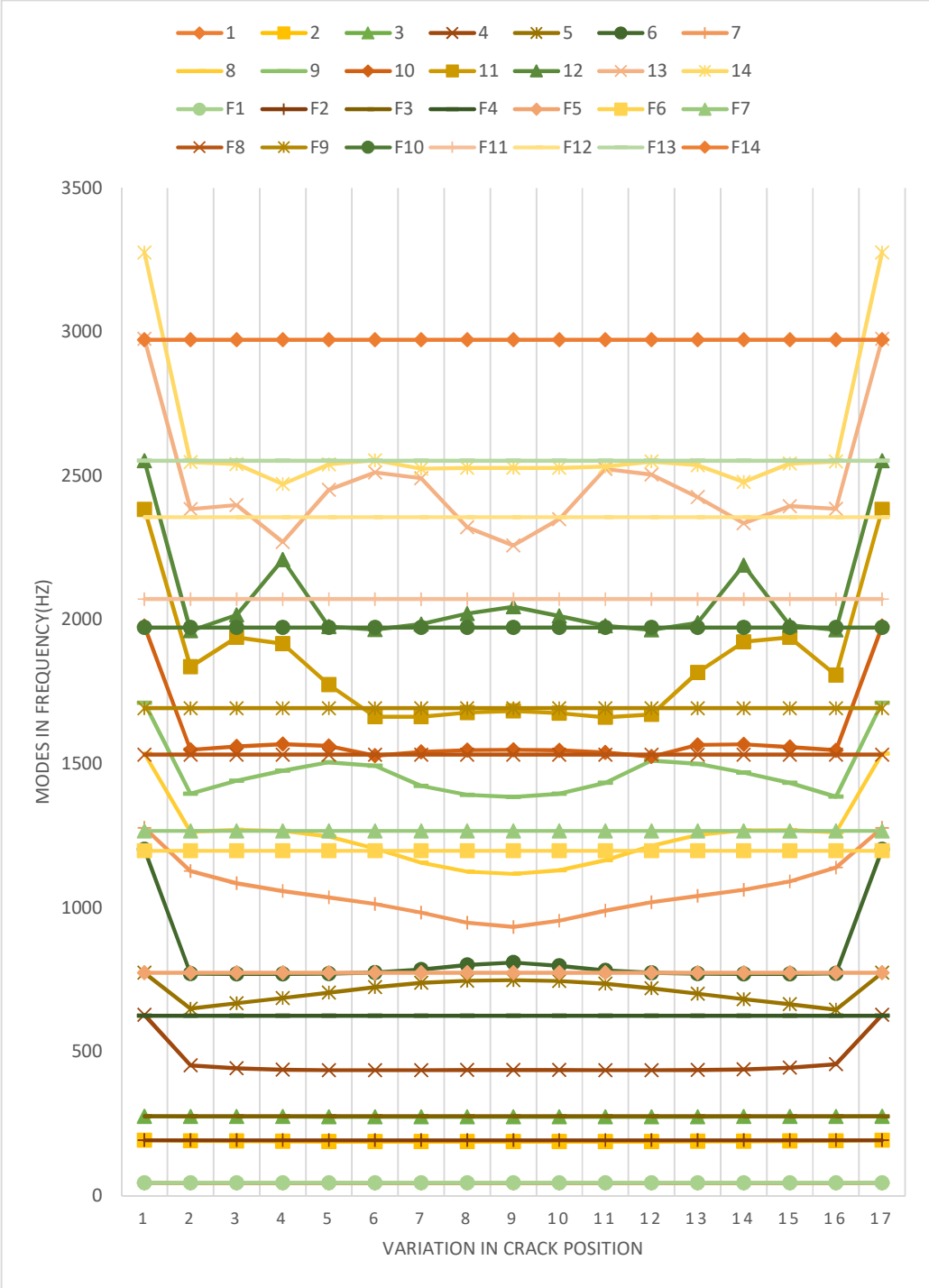

Figure 44: Mode Comparison of 123.75mm vertical crack ACE with flat plate

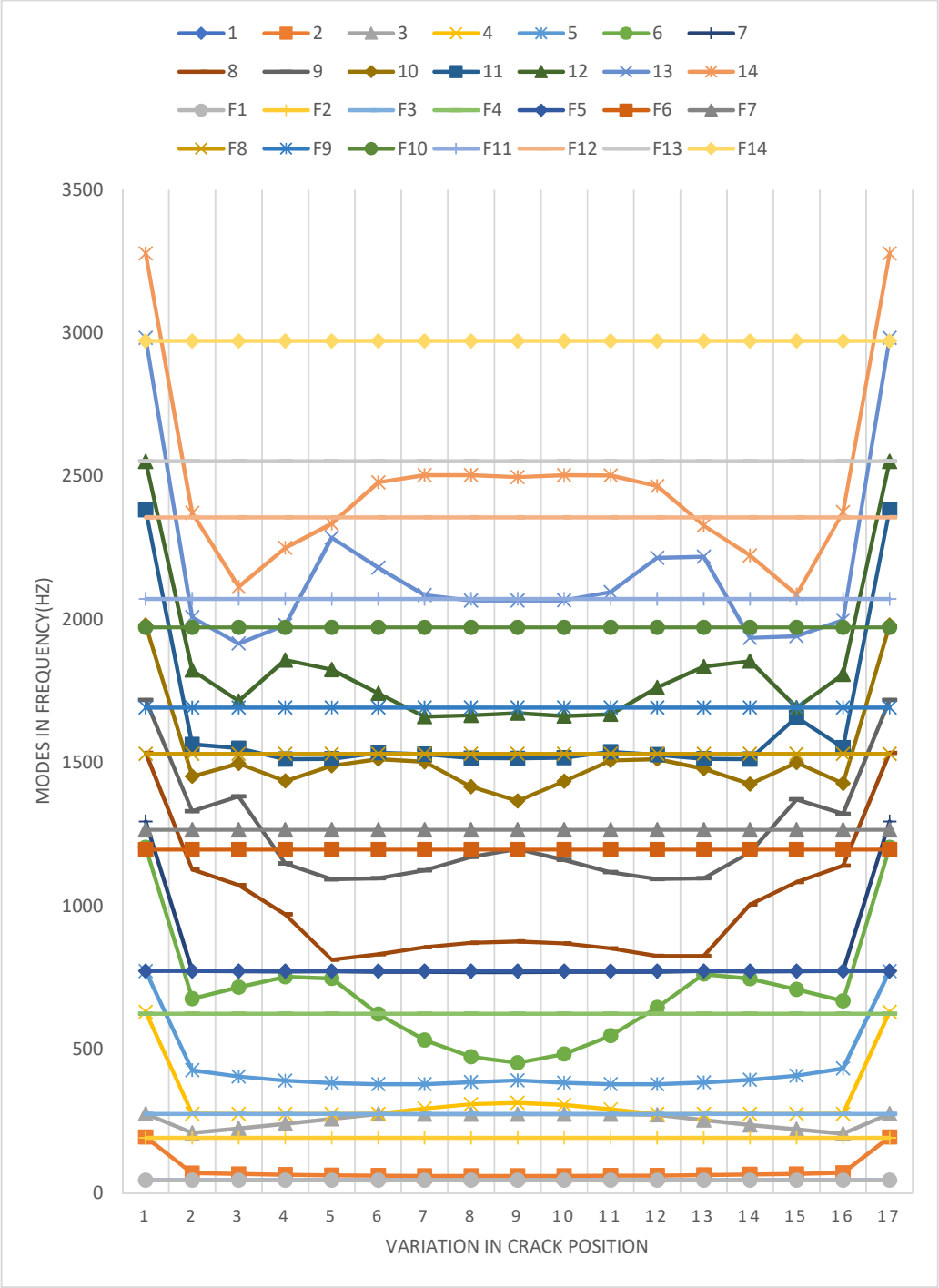

Figure 45: Mode Comparison of 123.75mm vertical crack AFE with flat plate

From the comparisons of the graphs of flat plate model with different type of cracks, the cracked model altogether having mode lines that are positioned averagely below than the uncracked flat plate. This is due to the material loss as the cracks are modeled as rectangular slits rather than cracks formed due to shear stress or by means which causes no noticeable material and internal structural deformities.

4.4.1 Finite Element Analysis Error Correction

Using the works of Nan Tao et al., it is seen that one or multiple data errors in modal frequency analysis might be present in the simulation with contrast to realistic results. This error can be rectified using mode shapes of the structure. These errors may be present for any cracked structure and at any frequency range with a higher probability of finding them in higher frequencies. In the defected mode shapes the displacement of the plate in any other axis is negligible.

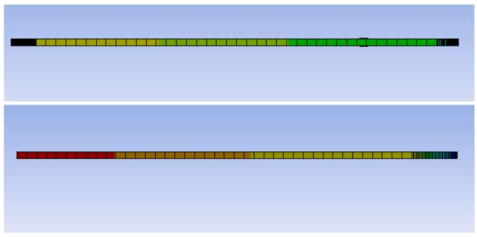

Figure 46: Mode shapes of error data seen from one side. Horizontal crack of 70 mm.

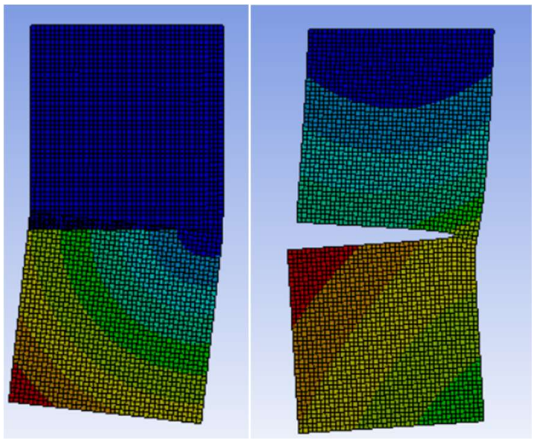

Figure 47: Mode shapes of error data seen from top. Horizontal crack of 70 mm.

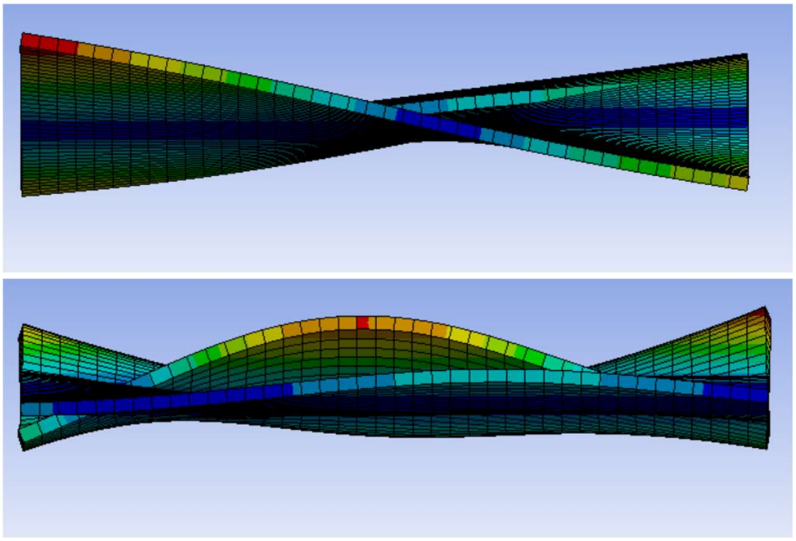

Figure 48: Correct mode shapes seen from the side. Horizontal crack of 70mm.

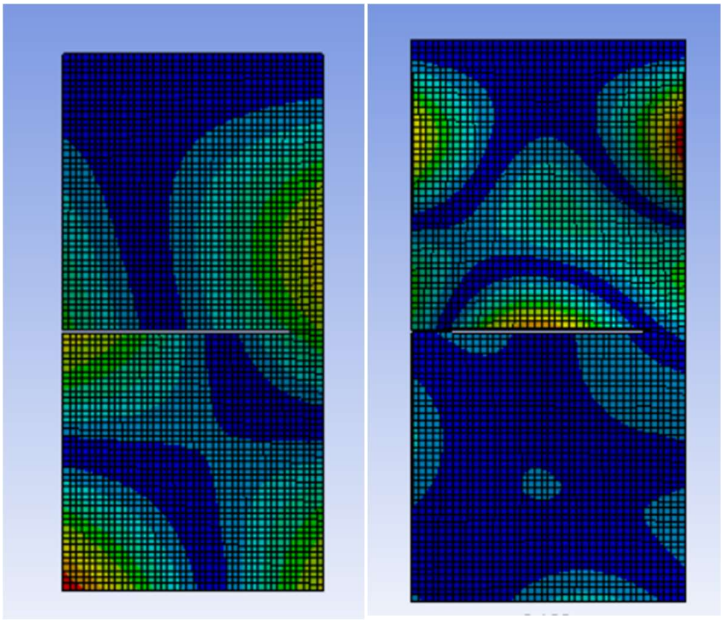

Figure 49: Correct mode shapes seen from top. Horizontal crack of 70mm.

4.4.2 Veering of Natural Frequency

From the works of Akira Saito and M.P. Castanier et al. the veering seen in the modal frequencies are due to the closing of the crack. At the veering regions fast mode switching is observed. Crack propagation at higher frequencies show more of these phenomena.

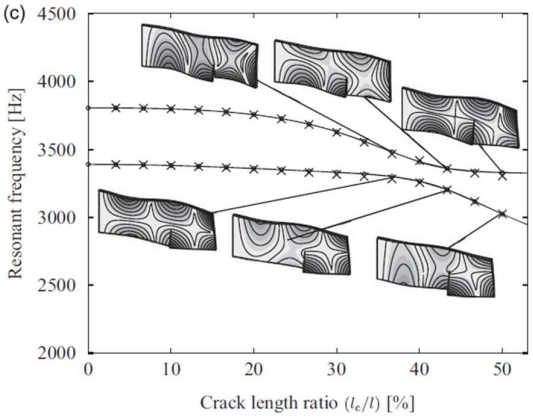

Figure 50: Veering seen from Analysis of Saito's work on slit position change

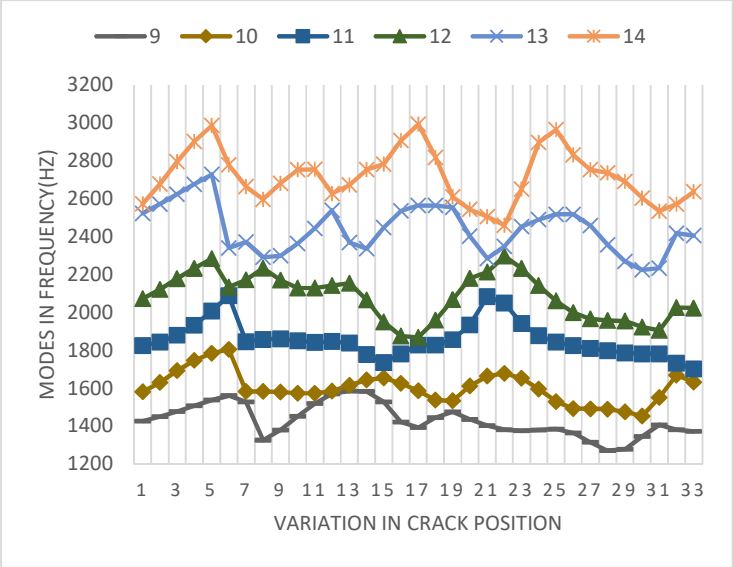

Figure 51: Veering seen from the results obtained by ANSYS

4.5 Harmonic Analysis

The harmonic analysis is done using 1N force at first for a horizontal crack of 70 mm along clamped edge. The simulation is run in a range 1 to 3500 hertz for an overall view. As 1N force is too much for a flat plate of this thickness, more simulations were done using .01N force. These were done between 25.2Hz to 225 Hz to capture the first three modes of this particular structure for a detailed view. The output found is plotted in displacement in mm vs frequency in Hertz. In the output, the points having sudden peaks are found to be in the modal frequencies. Although, a sudden depression is seen in the FIGURE 41, which is not in a modal point also, in an uncracked flat plate it should not be present.

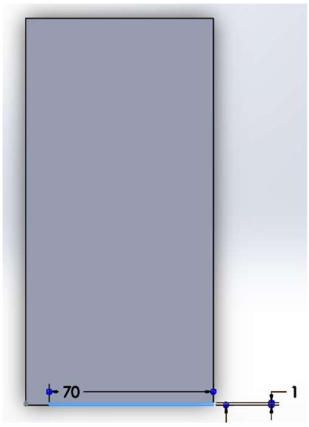

Figure 52: 70mm horizontally cracked plate

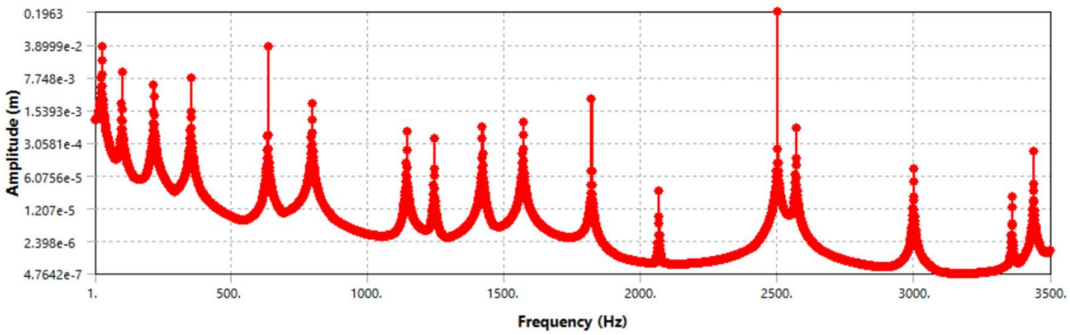

Figure 53: Frequency response of Harmonic Response of 70mm horizontally cracked plate using 1N force at the free edge

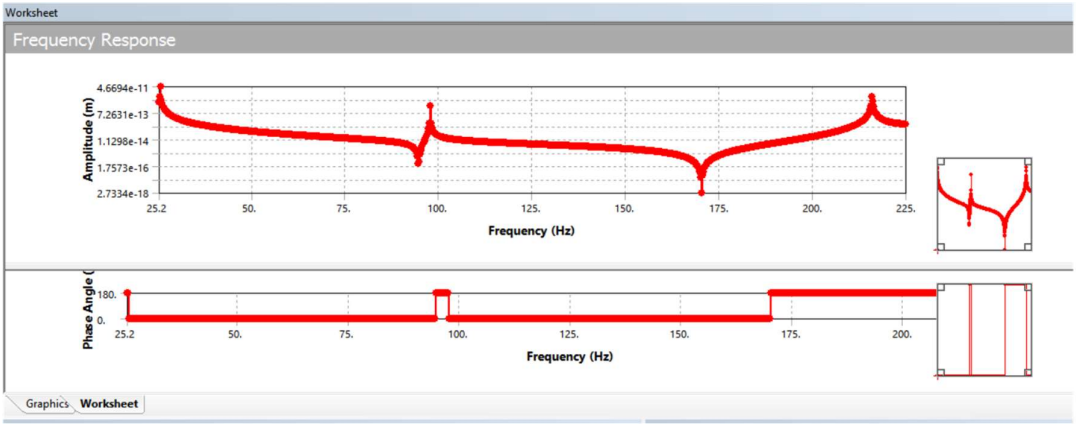

Figure 54: Frequency response of Harmonic Response of 70mm horizontally cracked plate using .01N force at the free edge

The frequency response of the analysis is similar to that of the works of Tanmoy Bose and Amiya R Mohanty. They have used variation in crack length and plotted a dimensionless response vs frequency.

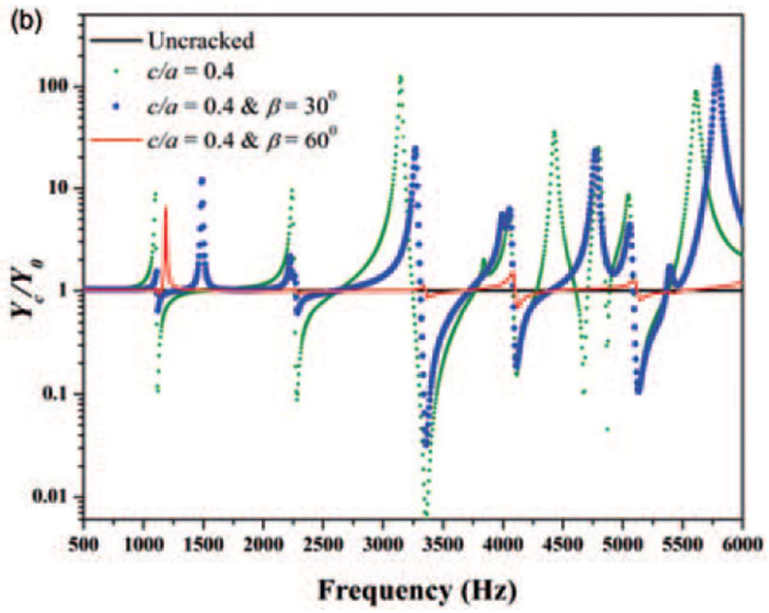

Figure 55: Frequency response from the work of Tanmoy et al.

5 Experimental Data

In the experimental procedure, the primary resources used are ECL 202e Eddy-current displacement sensor, a 1.5 mm thick Aluminum plate of required dimensions, a stainless-steel clamp and holder for the plate and sensor is used for vibration isolation, although for a small-scale structure such as this, more precautions and better isolation is needed still. The plate is excited using a very small amount of force remotely delivered to capture the first mode.

Figure 56: Experimental setup

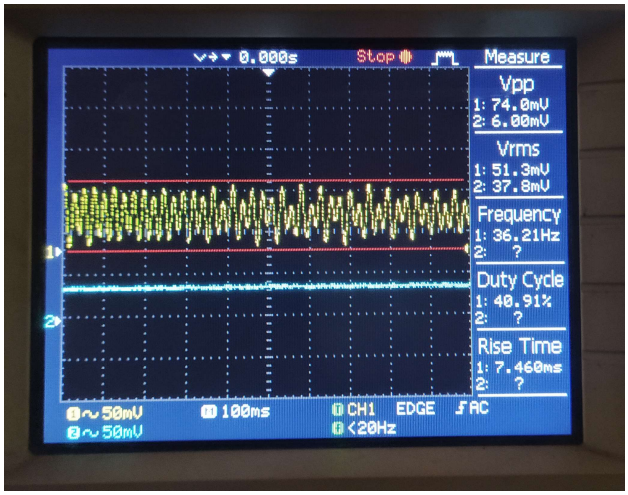

Figure 57(a): Experimental setup result

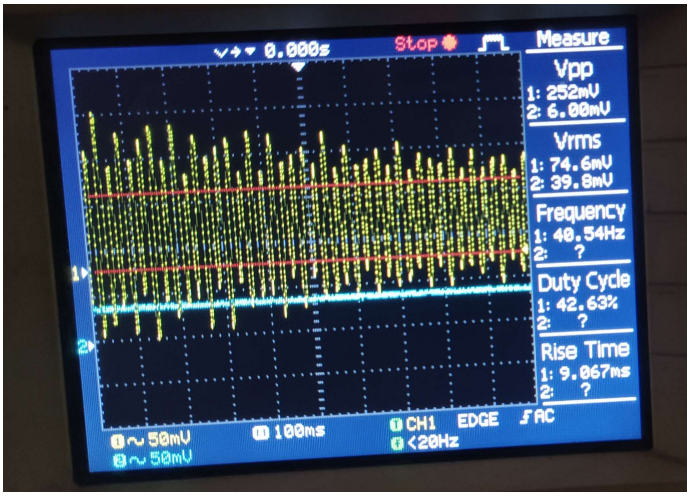

Figure 57(b): Experimental setup result

6 Result & Discussion

6.1 Validation

The results obtained from the ANSYS simulation is verified using the works of Nan Tao, Yinhang Ma, Hanyang Jiang et al. Observing under similar parameters, the variation in the output result is 0.49% in ANSYS 16.0. For a better fit in the result ANSYS is used for most of the simulations.

Mode	**FEM (Paper)**	**ESPI (Paper)**	**COMSOL Multiphysics**	**% Error**	**Ansys 16.0**	**% Error**
1	44.176	44.2	44.526	0.79	43.955	0.50
2	191.79	189.6	193.18	0.72	193.24	0.76
3	274.96	276.6	277.11	0.78	273.9	0.39
4	623.69	621.4	628.22	0.73	626.94	0.52
5	771.77	777.8	777.7	0.77	768.43	0.43
6	1195	1195	1203.7	0.73	1197.3	0.19
7	1265.2	1287.9	1274.1	0.70	1255.5	0.77
8	1527.8	1524.8	1539.1	0.74	1518	0.64
9	1690.4	1696.8	1702.3	0.70	1681.1	0.55
10	1968.4	1973.2	1982.7	0.73	1967.1	0.07
11	2353	2329.4	2368.6	0.66	2347.9	0.22
12	2546.2	2548.7	2564.5	0.72	2525.7	0.81
				0.73%		**0.49%**

Table 12: Simulation data comparison between paper and simulation interfaces.

In the experimental setup the results obtained are slightly less than that of the simulated data. This discrepancy may be due to the dimensional inaccuracy while machining the pieces, the lack of vibration isolation in the base of the sensor and plate holder, lack of soundproof environment and sensor data pick-up noise.

Experimental data (1st mode)	Average	Simulated Data (1st mode)	Error (%)
40.54	38.375	46.485	17.44%
36.21			

Table 13: Experimental data evaluation

The work of Koichi Maruyama et al.[15] states, that cracks emanating parallelly from the longer and shorter side slightly decreases the natural frequency slightly with an increase in length irrespective of its positioning. The cracks with inclinations of $\alpha=60^{o}$ show slightly increased frequency than that of $\alpha>60^{o}$ and then decreases with the inclination angle increase.

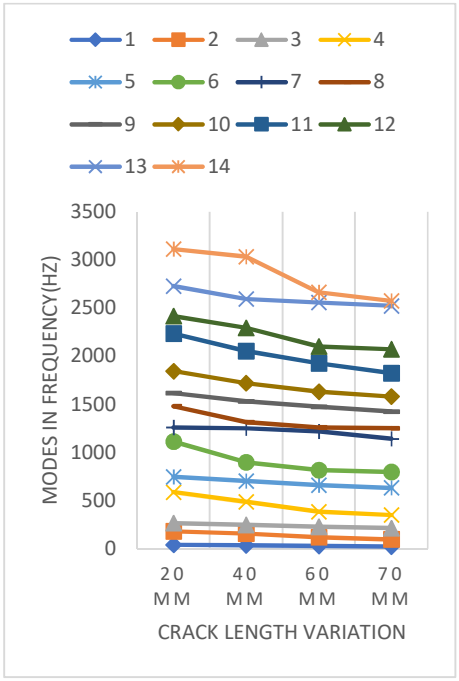

Figure 58: Modes vs crack length increase along the shorter side

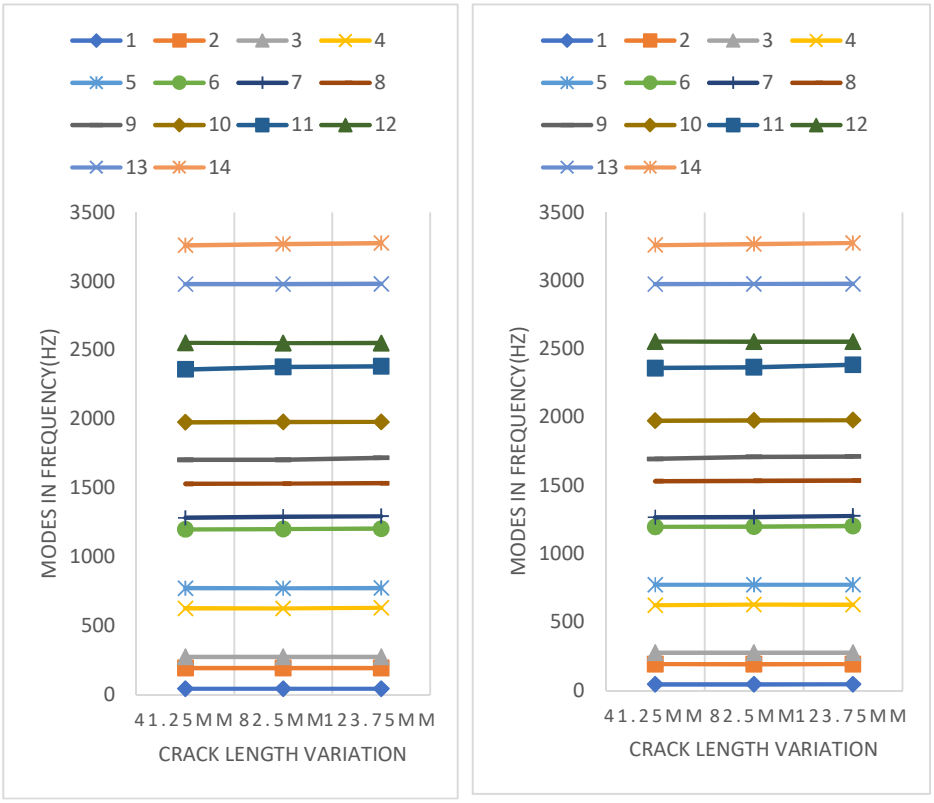

Figure 59: Modes vs crack length increase along the longer side for vertical crack AFE(a) and ACE(b)

The work done in the simulations also holds this to be true, especially for the first few modes. It is seen from our work also that the crack emanating parallelly from the shorter side shows decrease in natural frequency with the increase in length and for cracks emanating from longer side is seen to have little to no effect in natural frequency change with crack length change. In the work of Nan Tao, Hanyang Jiang et al. this phenomenon is seen also in their experiment and that too under the similar parameters of this work. The first case is therefore, validated.

7 Conclusion

This work presents an intensive insight into the behavior of a flat plate with different types of crack. The characteristics shown by the modal and harmonic analysis may well be used in further studies for other type of structures and crack types. Of many findings throughout the work, the important ones are as follows:

a) The natural frequency of the plate without any crack or slit is slightly higher than with any crack or slit in it. This is due to the material loss in the cracked models. There are two major types of crack analyzed, first type emanates parallelly along the clamped side and the other emanates vertically along the clamped side.

b) It is seen from the data available that modes in higher frequency shows more deviation with an increase in crack length. Increase in the crack length also shows more deviation in the data. Cracks at the edge of a structure provide higher modal frequencies than inside the structure.

c) There are errors found in FEM analysis in ANSYS while operating Modal Analysis. These errors were rectified using the work of Nan Tao, Hanyang Jiang et al. The errors are also observed and analyzed as to prevent from including wrong data in our studies.

d) The data found in the modal analysis are plotted in graphs and the variations in data are observed closely. The effects of varying crack's position and length are analyzed in the mode shapes and in the variation of modes in the graph.

e) This work also provides that cracks emanating from parallelly from the shorter side shows decrease in natural frequency with increase in crack length. This is also validated from the work of Koichi Maruyama and Osamu Ichinomiya.

f) In harmonic analysis the response in modal points are seen and certain depressions are seen which should not exist in an uncracked flat plate. Similarity in the charts have been found with the work of Tanmoy Bose and Amiya R. Mohanty.

g) In the experimental setup, the error found is approximately 17.447% This is due to lack of vibration isolation, soundproof environment and probably due to slight inaccuracy in dimensions while machining the part and noise pickup during signal processing.

Overall, this work provides an exclusive detail in case of cracks in a flat plate of the abovementioned variations.

8 Future Scopes

This work can provide insight into further crack propagation analysis for different shapes such as shells, beams, rods etc. Effect of crack for different shapes will always be different in all cases, but analyzing these might be able to provide for a better prediction of their behaviors. This study may be able to help exclusively in finding easier methods for crack detection using high precision displacement sensors or any other sensor for that matter. Crack prevention and further study for safety purposes could be possible. Studying about safety limit for load and vibration subjected on Turbomachinery is a must need in recent times as the number of Turbomachinery in power plants and high-end factories are rising globally. This study may be able to help in detecting cracks and their behavior under different loading. Also, due to higher frequency, crack generation may be prevented.

9 References

1. Dimarogonas, A.D. Vibration of cracked structures: A state of the art review. Eng. Fract. Mech. 1996, 55, 831–857.

2. Lynn, P.P.; Kumbasar, N. Free vibration of thin rectangular plates having narrow cracks with simply supported edges. Develop. Mech. 1967, 4, 911–928.

3. Stahl, B.; Keer, L.M. Vibration and stability of cracked rectangular plates. Int. J. Solids Struct. 1972, 8, 69–91.

4. Ali, R. and Atwal, S. (1980). Prediction of natural frequencies of vibration of rectangular plates with rectangular cutouts. Computers & Structures, 12(6), pp.819-823.

5. Huang, C.S.; Leissa, A.W.; Li, R.S. Accurate vibration analysis of thick, cracked rectangular plates. J. Sound Vib. 2011, 330, 2079–2093.

6. Maruyama, K.; Ichinomiya, O. Experimental study of free vibration of clamped rectangular plates with straight narrow slits. JSME Int. J. Ser. III 1989, 32, 187–193.

7. Bachene, M., Tiberkak, R. and Rechak, S. (2008). Vibration analysis of cracked plates using the extended finite element method. Archive of Applied Mechanics, 79(3), pp.249-262.

8. K.M. Liew, K.C. Hung, M.K. Lim, A solution method for analysis of cracked plates under vibration, Eng. Fract. Mech. 48 (3) (1994) 393–404.

9. Bose, T. and Mohanty, A. (2014). Detection and monitoring of side crack in a rectangular plate using mobility. Journal of Vibration and Control, 22(2), pp.585-594.

10. Tao, N., Ma, Y., Jiang, H., Dai, M. and Yang, F. (2018). Investigation on Non-Linear Vibration Response of Cantilevered Thin Plates with Crack Using Electronic Speckle Pattern Interferometry. Proceedings, 2(8), p.539.

11. Qiu, Z., Wu, H. and Ye, C. (2009). Acceleration sensors based modal identification and active vibration control of flexible smart cantilever plate. Aerospace Science and Technology, 13(6), pp.277-290.

12. Andreaus, U. and Baragatti, P. (2012). Experimental damage detection of cracked beams by using nonlinear characteristics of forced response. Mechanical Systems and Signal Processing, 31, pp.382-404.

13. Saito, A.; Castanier, M.P.; Pierre, C. Estimation and veering analysis of nonlinear resonant frequencies of cracked plates. J. Sound Vib. 2009, 326, 725–739.

14. Elshamy, M., Crosby, W. and Elhadary, M. (2018). Crack detection of cantilever beam by natural frequency tracking using experimental and finite element analysis. *Alexandria Engineering Journal,* 57(4), pp.3755-3766.

15. MARUYAMA, K. and ICHINOMIYA, O. (1989). Experimental study of free vibration of clamped rectangular plates with straight narrow slits. *JSME international journal. Ser. 3, Vibration, control engineering, engineering for industry*, 32(2), pp.187-193.